# Edge integration and the perception of brightness and darkness

Vladusich, Tony; Lucassen, Marcel P.; Cornelissen, Frans W.

*Published in:*
JOURNAL OF VISION

*DOI:*
10.1167/6.10.12

# Edge integration and the perception of brightness and darkness

**Tony Vladusich**

Laboratory of Experimental Ophthalmology & NeuroImaging Centre, School of Behavioural and Cognitive Neurosciences, University Medical Centre Groningen, Groningen, The Netherlands

**Marcel P. Lucassen**

Department of Human Interfaces, TNO Human Factors, Soesterberg, The Netherlands

**Frans W. Cornelissen**

Laboratory of Experimental Ophthalmology & NeuroImaging Centre, School of Behavioural and Cognitive Neurosciences, University Medical Centre Groningen, Groningen, The Netherlands

How do induced brightness and darkness signals from local and remote surfaces interact to determine the final achromatic color percept of a target surface? An emerging theory of achromatic color perception posits that brightness and darkness percepts are computed by weighting and summing the induction signals generated at edges in a scene. This theory also characterizes how neighboring edges interact to modulate the gain of brightness and darkness signals induced from one another. Here we assess evidence for this edge integration theory by means of computational modeling and a psychophysical experiment. We quantitatively show how local and remote edge induction signals in disk-ring displays give rise to either contrast or assimilation effects. Spatial integration of same-polarity edge signals supports a contrast effect, whereas integration of opposite-polarity signals supports an assimilation effect, particularly when the remote induction signal is much stronger than the local induction signal. The results confirm a key prediction of edge integration theory, namely, that strong assimilation effects can lead subjects to ignore the polarity of local edge information when setting achromatic color matches. The conditions necessary for strong assimilation effects are also associated with greater difficulty in setting matches, suggesting that caution is required when interpreting matching data in terms of gain control. We describe several avenues for further study of contrast, assimilation, and gain control.

Keywords: contrast, assimilation, brightness, darkness, integration, edge

## Introduction

The achromatic color (perceived luminance) of a surface depends both on its own luminance and that of nearby surfaces. An adjacent surface of lower luminance than the surface of interest will induce brightness, whereas one with a higher luminance than the target will induce darkness. Here, our goal is to understand how such induction signals from local and remote surfaces interact to determine a final achromatic color percept. Land and McCann (1971) introduced retinex theory in an attempt to quantitatively model properties of human chromatic and achromatic color constancy. Applied to brightness and darkness perception, their theory posits that the brain discounts global illumination changes by summing induction signals computed at edges in a scene. Shapley and Reid (1985) studied the spatial integration of edge induction signals in psychophysical matching experiments involving displays containing a central disk surrounded by rings of identical luminance placed on different backgrounds. The authors discussed evidence for two induction processes: a strong *contrast* process—acting to reduce the similarity between target and ring—and a weaker *assimilation* process (Helson, 1963)—acting to increase the similarity between target and ring.

Rudd et al. (Rudd & Arrington, 2001; Rudd & Zemach, 2004, 2005) have recently developed a systematic quantitative approach to understanding the relationship between contrast and assimilation in achromatic color perception (Bindman & Chubb, 2004; Blakeslee & McCourt, 2004; Blakeslee, Pasieka, & McCourt, 2005; De Weert & Spillmann, 1995; Güçlü & Farell, 2005; Hong & Shevell, 2004a, 2004b; Howe, 2005; Rudd & Arrington, 2001; Rudd & Zemach, 2004, 2005; Shapley & Reid, 1985; Vladusich, Lucassen, & Cornelissen, 2006). The theory interprets contrast and assimilation as complementary *effects* rather than distinct *processes*. On the one hand, the theory predicts that a *pure contrast effect* arises when the local and remote inducers share the same contrast

doi: 10.1167/6.10.12 Received January 13, 2006; published September 29, 2006 ISSN 1534-7362 

polarity. On the other hand, the theory predicts that a remote edge manifesting the opposite polarity to the local edge induces a *partial assimilation effect*. The assimilation effect is only partial because the local edge generates a competing contrast effect. The balance between these contrast and assimilation effects depends on the relative strengths of the local and remote induction signals. Aside from the distance between local and remote edges (Rudd & Arrington, 2001; Rudd & Zemach, 2004; Zaidi, Yoshimi, Flanigan, & Canova, 1992), one important factor in determining the balance between contrast and assimilation effects is the physical contrast of the remote edge relative to the physical contrast of the local edge. We show here empirically that when the contrast of the remote edge is high and the contrast of the local edge low, a remote assimilation effect can completely overwhelm any local contrast effect.

The edge integration theory also posits the existence of a *gain control process,* whereby the influence of remote induction signals is modulated by the strength of local edge signals (Rudd & Arrington, 2001). In a disk-ring configuration, for example, the local edge of the display is posited to *partially block* induction signals originating at the remote edge. The strength of the blocking is proportional to the contrast of the local edge: high contrast implies less contribution of the remote edge to the brightness or darkness of the target surface. Although we refer to this process in a general way as gain control, it is important to keep in mind that evidence specifically favoring the blocking interpretation must necessarily involve a *reduction* in the magnitude of the induction signal.

Here we study the interactions among contrast, assimilation, and gain control effects through computational modeling and psychophysical experiments. The first part of this paper aims to characterize how the strength of gain control effects varies with the conditions supporting either contrast or assimilation effects. We conduct a modeling study on published data (Hong & Shevell, 2004a, 2004b) to examine the polarity specificity of gain control between edges and to quantify evidence for the blocking interpretation (Figure 1). These results set the stage for the second part of the paper, in which we employ both psychophysical and modeling methods to test specific predictions of the edge integration theory concerning contrast, assimilation, and gain control.

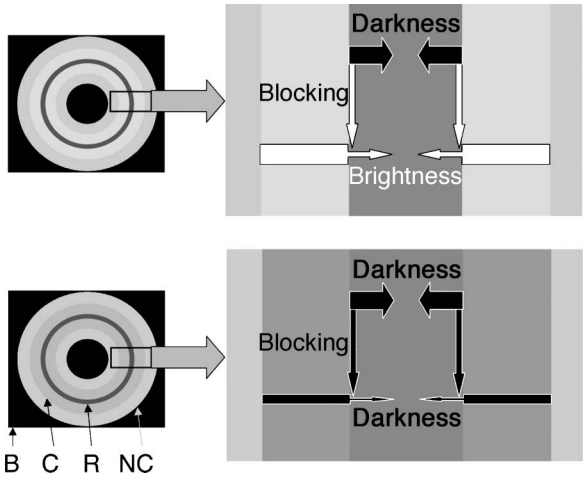


Figure 1. Illustration of the interactions among contrast, assimilation, and gain control (blocking) effects. The figure is based on stimuli used in the study of Hong and Shevell (2004b). The local edge, formed by the reference ring (R) and contiguous ring (C), induces darkness (thick black arrows) signals into the reference ring in the middle of the concentric-ring configuration. The remote edge, formed by the contiguous and noncontiguous rings (NC), induces either darkness (thin black arrows) or brightness (thin white arrows) depending on the polarity of the remote edge. The arrows emanating from the remote edge have different thicknesses to illustrate that they can, in principle, be weighted by different factors. Both types of induction signal are modulated by the putative blocking (more generally, gain control) signals generated at the local edge. Blocking decreases the strength of the induction signal, as indicated by the thinning of the arrows representing induction signals from the remote edge as they pass through the local edge. The gain control signals can, in principle, be weighted differently for different polarities of the remote edge. This fact is illustrated by the white and black arrows used in the upper and lower panels, where remote-edge polarities differ. A range of simpler models can be derived from this general model by simply constraining the model parameters in various ways (Figure 2). It is important to note that a contrast effect will always arise when local and remote inducers share the same polarity (Rudd & Arrington, 2001), whereas either a contrast effect or an assimilation effect can emerge when the remote signal is opposite in polarity to the local edge (Rudd & Zemach, 2004; Shapley & Reid, 1985).

## Modeling of published data

A previous study in which local and remote edges shared the same polarity provided strong evidence in favor of blocking (Rudd & Arrington, 2001), whereas a study using opposite-polarity edges produced mixed results (Rudd & Zemach, 2004). In the first part of the paper, we aim to characterize evidence for the polarity specificity of blocking effects under conditions which support either a pure contrast effect—when local and remote edges share the same polarity—or an assimilation effect—when local and remote edges manifest the opposite polarity (Hong & Shevell, 2004a, 2004b).

Hong and Shevell (2004b) demonstrated that the range of spatial integration is broader when remote induction edges are luminance decrements than when they are increments (the local edge was always a darkness-inducing decrement). This observation suggests that different

distance-dependent weighting functions underlie the integration of brightness and darkness. Here we model these differential weighting functions in terms of half-wave rectified (HWR) channels (Beer & MacLeod, 2000; Bindman & Chubb, 2004; Elder & Sachs, 2004; Rudd & Zemach, 2004, 2005; Sankeralli & Mullen, 2001; Vladusich et al., 2006). Edge signals are first encoded as log luminance ratios (Land & McCann, 1971; Rudd & Arrington, 2001) before being differentially weighted according to edge polarity. Half-wave rectification ensures that induction signals associated with only one polarity may be active at any given location. Similarly, the blocking signal itself can be made polarity specific or nonspecific by setting the values of the gain parameters associated with opposite-polarity induction signals in an appropriate way.

In another report, Hong and Shevell (2004a) studied how the darkness of a target surface is related to the luminance of a contiguous region. They found an inverted-U (or nonmonotonic) relationship between luminance and darkness when the local and remote borders of the display shared the same polarity (i.e., both were darkness-inducing decrements). The relationship between perceived darkness and the luminance of the contiguous region was, in comparison, found to be linear when the local and remote edges manifested opposite polarities (i.e., the local edge was a decrement and the remote edge an increment). Hong and Shevell (2004a) thereby provided qualitative evidence that the inverted-U function is specifically associated with conditions necessary for a pure contrast effect. The authors proved mathematically that the inverted-U function can be explained as a blocking effect in edge integration theory, although no computational analyses were presented.

To examine the nature of any putative blocking effects in these data sets, we construct a suite of models (Figure 2) in which induction and gain control signals (i.e., gain control can either block or enhance the induction signal, depending on the estimated parameter values) are defined by HWR brightness and darkness channels (Bindman & Chubb, 2004; Rudd & Zemach, 2005; Vladusich et al., 2006). All the models are derived by placing specific constraints on the weighting parameters associated with induction and gain control signals (see Methods).

These models are individually fit to the published data. Model *performance* is computed using statistical techniques, known as Akaike's information criterion and the Bayesian information criterion (Burnham & Anderson, 2002), which quantify the trade-off between the number of fitted parameters in each model and the quality of the fits. A wide variety of models are tested to exclude the possibility of incorrectly concluding that gain control is absent due to the use of an unnecessarily complex gain control model. We additionally implement an alternative model that incorporates gain control but cannot be conceptualized in terms of a blocking process.

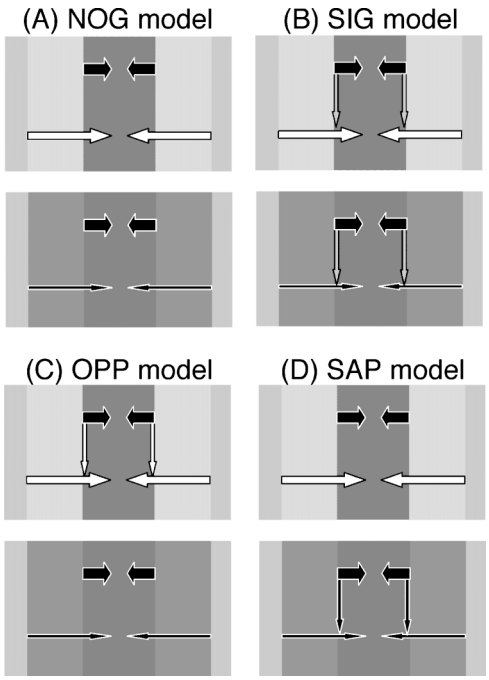


Figure 2. A suite of models derived from the general theory of HWR brightness and darkness channels (Figure 1) by constraining the model parameters in various ways. (A) The NOG model. The white and black pathways from the remote edge are weighted by different functions (denoted by having different thicknesses) but are not gain controlled by the local edge. (B) The single-polarity gain (SIG) model. The remote-edge induction pathways are both gain controlled by the same signal from the local edge. (C) The OPP model. Gain control is restricted to remote edges with the opposite polarity to the local edge. (D) The SAP model. Gain control is restricted to remote edges with the same polarity as the local edge.

## New psychophysical data and further modeling

We conducted an achromatic color-matching experiment, using a disk-ring configuration, to provide additional information about the nature of contrast, assimilation, and blocking effects. Unlike previous studies (Hong & Shevell, 2004a, 2004b; Rudd & Arrington, 2001; Rudd & Zemach, 2004), we systematically varied the polarity of *both* local- and remote-inducing edges in a single experiment. The main aim of the experiment was to test a key prediction of the edge integration theory. Specifically, the theory predicts that an assimilation effect induced by a remote edge of appropriate polarity can completely overwhelm the contrast effect of a local edge. Under such conditions, subjects should adjust the luminance of a matching disk

on a uniform background to match the polarity of the remote inducer rather than the local inducer. Because the local contrast effect is substantially weaker than the remote assimilation effect, subjects should ignore the polarity of the local reference edge when setting the polarity of the matching disk with respect to its immediate surround. Because subjects usually avoid making such increment–decrement and decrement–increment matches (Whittle, 1994), the prediction is somewhat counter-intuitive.

In our experiment, subjects also rated the difficulty of making each match on a 1–10 scale. The rating task allows us to examine whether matches in which subjects ignore local edge polarity are more difficult to set than increment–increment and decrement–decrement matches. We expect that the former matches are more difficult to make because ignoring local polarity information is tantamount to making a setting in which the matching disk may "not look quite right" (Whittle, 1994). The issue of whether achromatic color matches are always possible (Logvinenko & Maloney, 2006)—particularly when local and remote edges have the opposite polarity (Faul, Ekroll, & Vladusich, 2006)—may help to resolve conflicting reports concerning the conditions under which blocking does and does not occur (Rudd & Arrington, 2001; Rudd & Zemach, 2004).

# Methods

## Description of Hong–Shevell experiments

We provide here sufficient details of the experimental set up used by Hong and Shevell, (2004a, 2004b) to motivate the modeling study. The interested reader is referred to the original publications for further details. Subjects in Hong and Shevell (2004b) adjusted the luminance of a *matching* ring to appear the same brightness as a *reference* ring. The matching ring was surrounded by a contiguous ring whose luminance values stayed constant throughout the experiment (24 cd/m$^2$). The reference ring was surrounded by two concentric rings and a background of identical luminance to that surrounding the matching rings. The luminance of the reference ring was kept constant whereas the luminance of the ring directly adjacent to the reference ring—the contiguous ring—was varied. The width of the contiguous ring was also varied in eight steps such that it occupied a variable amount of space between the reference ring and the noncontiguous ring (the ring surrounding the contiguous ring).

The stimuli used in Hong and Shevell (2004a) were similar to those in Hong and Shevell (2004b), with the caveat that the former study made use of four rings surrounding the reference ring rather than two (contiguous and noncontiguous rings were interleaved in the former). To simplify our modeling, we shall assume that the stimuli were identical in the two psychophysical studies. In Hong and Shevell (2004a), the width of the contiguous ring remained fixed (at 8° visual angle). The luminance of the noncontiguous ring remained fixed at either 16 or 24 cd/m$^2$, whereas the luminance of the contiguous ring varied over a range from 18 to 24 cd/m$^2$ in steps of 2 cd/m$^2$. We also model two control conditions in Hong and Shevell (2004a). In one condition, the contiguous and noncontiguous rings were replaced by a single (solid) ring varying from 18 to 24 cd/m$^2$. In the other, the luminance of the contiguous ring remained constant at 24 cd/m$^2$ whereas the luminance of the noncontiguous ring varied from 18 to 24 cd/m$^2$.

## General theory

We first write the most general form of the modeling equation, then simplify the equation to describe our modeling of the Hong–Shevell studies. For simplicity, we assume that the edge formed by the contiguous and background surfaces does not contribute significantly to the achromatic color of the matching ring. This assumption is justified by the data of Hong and Shevell, (2004a, 2004b), who reported only a minor effect of the remote edge in the reference display at the distance used in the matching display. For the matching display, we have

$$x_m = w_{\mathrm{B}}^{\mathrm{L}}\left[\log\frac{T_m}{C_m}\right]^{+} - w_{\mathrm{D}}^{\mathrm{L}}\left[\log\frac{C_m}{T_m}\right]^{+} + c, \qquad (1)$$

where $x_m$ is the neural activity associated with the target surface in the matching display (ring in Hong–Shevell, disk in the current experiments), and $T_m$ and $C_m$ represent the luminance values of the target and contiguous regions of the matching display. As indicated previously, the edge signals are computed as log luminance ratios, which are HWR to mimic the neural constraint that negative spike rates are impossible. The HWR notation, $[y]^+ = \max(z, 0)$, implies a physical mechanism that substitutes for the inversion of log luminance ratios with opposite-polarity combinations of local and remote edges (Rudd & Zemach, 2004). The constant, $c$, is assumed to be large and positive, ensuring that $x_m > 0$, whereas $w_{\mathrm{B}}^{\mathrm{L}}$ and $w_{\mathrm{D}}^{\mathrm{L}}$ correspond to real positive weights applied to opposite-polarity edges of the matching display. The superscript (L) indicates that the position of the edge corresponds to the position of the local edge in the reference display, whereas the subscripts (B, D) denote whether the target is matched

as an increment (B for bright) or decrement (D for dark). We adopt the arbitrary convention of denoting decrements as negative.

Because subjects in Hong and Shevell, (2004a, 2004b) always made matches that satisfy the constraint $T_m < C_m$, we may implement only the darkness term, removing the half-wave rectification brackets, and inverting the log luminance ratio and the sign of the term

$$x_m = w_{\mathrm{D}}^{\mathrm{L}} \log \frac{T_m}{C_m} + c. \tag{2}$$

For the reference display we have a more complex expression

$$\begin{aligned} x_r \;=\; & w_{\mathrm{B}}^{\mathrm{L}} \left[\log \frac{T_r}{C_r}\right]^+ - w_{\mathrm{D}}^{\mathrm{L}} \left[\log \frac{C_r}{T_r}\right]^+ + w_{\mathrm{B}}^{\mathrm{R}} \left[\log \frac{C_r}{NC_r}\right]^+ \\ & \times \left(1 - g_{\mathrm{B}}^{\mathrm{B}} \left[\log \frac{T_r}{C_r}\right]^+\right) \left(1 - g_{\mathrm{D}}^{\mathrm{B}} \left[\log \frac{C_r}{T_r}\right]^+\right) \\ & - w_{\mathrm{D}}^{\mathrm{R}} \left[\log \frac{NC_r}{C_r}\right]^+ \left(1 - g_{\mathrm{D}}^{\mathrm{B}} \left[\log \frac{T_r}{C_r}\right]^+\right) \\ & \times \left(1 - g_{\mathrm{D}}^{\mathrm{D}} \left[\log \frac{C_r}{T_r}\right]^+\right) + c, \end{aligned} \tag{3}$$

where $x_r$ is the neural activity associated with the target surface, and $T_r$, $C_r$, and $NC_r$ represent the luminance values of the reference target, contiguous region, and noncontiguous region, respectively. Equation 3 says that the local edge induction signals and the gain-controlled remote induction signals additively interact to determine achromatic surface color. The superscripts and subscripts associated with the gain control parameters, $g = \{g_{\mathrm{B}}^{\mathrm{B}}, g_{\mathrm{D}}^{\mathrm{B}}, g_{\mathrm{D}}^{\mathrm{D}}, g_{\mathrm{B}}^{\mathrm{D}}\}$, denote the polarity of the remote and local edges, respectively. Each gain control parameter therefore specifies a unique polarity relationship between local and remote induction signals. Half-wave rectification ensures that only certain terms are simultaneously active. Consider, for example, the Hong–Shevell display, in which the local edge induces darkness and the remote edge induces either brightness or darkness. Equation 3 then reduces to

$$\begin{aligned} x_r = & -w_{\mathrm{D}}^{\mathrm{L}} \left[\log \frac{C_r}{T_r}\right]^+ \\ & + w_{\mathrm{B}}^{\mathrm{R}} \left[\log \frac{C_r}{NC_r}\right]^+ \left(1 - g_{\mathrm{D}}^{\mathrm{B}} \left[\log \frac{C_r}{T_r}\right]^+\right) \\ & - w_{\mathrm{D}}^{\mathrm{R}} \left[\log \frac{NC_r}{C_r}\right]^+ \left(1 - g_{\mathrm{D}}^{\mathrm{D}} \left[\log \frac{C_r}{T_r}\right]^+\right) \end{aligned} \tag{4}$$

because the local brightness term becomes equal to zero and because all irrelevant gain control terms become equal to one. Equation 4 can be rewritten as

$$\begin{aligned} x_r = & w_{\mathrm{D}}^{\mathrm{L}} \log \frac{T_r}{C_r} + w_{\mathrm{B}}^{\mathrm{R}} \left[\log \frac{C_r}{NC_r}\right]^+ \left(1 - g_{\mathrm{D}}^{\mathrm{B}} \log \frac{T_r}{C_r}\right) \\ & - w_{\mathrm{D}}^{\mathrm{R}} \left[\log \frac{NC_r}{C_r}\right]^+ \left(1 - g_{\mathrm{D}}^{\mathrm{D}} \log \frac{T_r}{C_r}\right). \end{aligned} \tag{5}$$

The terms, $\left[\log \frac{C_r}{NC_r}\right]^+$ and $\left[\log \frac{NC_r}{C_r}\right]^+$ represent the brightness and darkness induction signals associated with the remote inducer. The term $\left(1 - g_{\mathrm{D}}^{\mathrm{B}} \log \frac{C_r}{T_r}\right)$ represents the signal, originating from the local edge, that controls the gain of brightness induction from the remote edge, whereas the term $\left(1 - g_{\mathrm{D}}^{\mathrm{D}} \log \frac{C_r}{T_r}\right)$ gain controls the darkness signal from the remote edge. The gain control parameters must be positive to be consistent with an interpretation in terms of the partial blockage of induction signals (Rudd & Zemach, 2004). In other words, the products of the weighted gain control and induction terms must always be *less than* the weighted induction signals themselves to be interpreted in terms of blocking. In the Hong–Shevell experiments, subjects set the matching luminance by satisfying the identity $x_m = x_r$. Thus, by setting Equation 2 equal to Equation 5, we derive the following expression

$$\begin{aligned} \log T_m = & \log \frac{T_r C_m}{C_r} + \frac{w_{\mathrm{B}}^{\mathrm{R}}}{w_{\mathrm{D}}^{\mathrm{L}}} \left[\log \frac{C_r}{NC_r}\right]^+ \left(1 - g_{\mathrm{D}}^{\mathrm{B}} \log \frac{T_r}{C_r}\right) \\ & - \frac{w_{\mathrm{D}}^{\mathrm{R}}}{w_{\mathrm{D}}^{\mathrm{L}}} \left[\log \frac{NC_r}{C_r}\right]^+ \left(1 - g_{\mathrm{D}}^{\mathrm{D}} \log \frac{T_r}{C_r}\right), \end{aligned} \tag{6}$$

which can be rewritten as

$$\begin{aligned} \log\ T_m = & \log \frac{T_r C_m}{C_r} + w_{\mathrm{D}}^{\mathrm{B}} \left[\log \frac{C_r}{NC_r}\right]^+ \left(1 - g_{\mathrm{D}}^{\mathrm{B}} \log \frac{T_r}{C_r}\right) \\ & - w_{\mathrm{D}}^{\mathrm{D}} \left[\log \frac{NC_r}{C_r}\right]^+ \left(1 - g_{\mathrm{D}}^{\mathrm{D}} \log \frac{T_r}{C_r}\right), \end{aligned} \tag{7}$$

adopting the same subscript–superscript notation as used for the gain parameters. For modeling of the Hong and Shevell (2004b) data, the weighting parameters are defined by the following generalized exponential distance-dependent weighting function (Zaidi et al., 1992)

$$w = ke^{-md}. \tag{8}$$

Here $d$ is the distance between the local and remote edges in degrees of visual angle (we obtained the same results with angular or Cartesian distance), $k$ controls the

height of the exponential function, whereas $m$ controls the rate of decrease of the function with distance. From Equation 7, the matching luminance, $T_m$, is equal to $10^{\log T_m}$.

We separately tested another gain control model on the Hong–Shevell data. This model is defined as

$$\log T_m = \log C_m + \log \frac{T_r}{C_r}\left(1 - g_D^B\left[\log \frac{C_r}{NC_r}\right]^+\right) \times \left(1 - g_D^D\left[\log \frac{NC_r}{C_r}\right]^+\right) + w_D^B\left[\log \frac{C_r}{NC_r}\right]^+ - w_D^D\left[\log \frac{NC_r}{C_r}\right]^+ \quad (9)$$

and cannot be interpreted in terms of blocking because the remote induction signal controls the gain of the local induction signal, rather than vice versa.

## Polarity-constrained models of the Hong–Shevell experiments

The theory above was used to generate a suite of five models (Figure 2). Each model represents a different constraint on the way edges of different polarities interact. The most general model (Figure 1), the *unconstrained polarity gain* (UP) model, represents the hypothesis that remote induction signals of either polarity are gain controlled by the local edge with potentially different strengths ($w_D^D$ and $w_D^B$ vary freely). This model has either 4 or 6 parameters, depending on which Hong–Shevell study we model. Another model corresponds to the simplest possible constraint: that there is no gain control ($w_D^D = w_D^B = 0$). We refer to this model as the *no-gain* (NOG) model (Figure 2A). This model has the fewest free parameters (2 or 4). The *single-gain* (SIG) model (Figure 2B) tests the hypothesis of a single-gain signal associated with both polarities of the remote induction signal ($w_D^D = w_D^B$) (3 or 5 parameters). The *opposite-polarity gain* (OPP) model (Figure 2C) represents the hypothesis of opposite-polarity gain control ($w_D^D = 0$) (3 or 5 parameters). In the *same-polarity gain* (SAP) model (Figure 2D), the incremental gain parameter is constrained to zero ($w_D^B = 0$). This model represents the hypothesis that gain control occurs only for same-polarity edges (3 or 5 parameters).

## Fitting

We fit the models and produce confidence intervals on fitted data points and parameters by means of a nonlinear least squares optimization procedure. This fitting procedure made use of the *nlnfit* and *lsqcurvefit* functions of Matlab (Version 7.0.4, The MathWorks Inc.), whereas 95% confidence intervals on estimated parameters and data points were computed with the *nlpredci* and *nlparci* functions. All models usually converged well, often generating extremely high values for the variance explained ($R^2 > 95\%$), where

$$R^2 = 100\left(1 - \frac{SS_{fit}}{SS_{total}}\right) \quad (10)$$

where $SS_{fit}$ is the sum-of-squares derived from the fit, and $SS_{total}$ is the sum-of-squares derived from a flat line determined by the mean of the residuals. We attempted to obtain better fits by randomly toggling the starting parameter values, but we could not obtain better fits than those obtained with starting values of zero. We therefore conclude that the convergence solutions are likely to represent global, rather than local, minima. For modeling of the Hong–Shevell data, the few cases where a model did not converge within 50 iterations are indicated in the data tables. Increasing the number of iterations to 250 only improved the fit at a level of two decimals points of the $R^2$ value in one case (see Table 2).

The $R^2$ values derived for each subject in our study were always close to 100%. Because $R^2$ is asymptotic, large improvement in the sum-of-squares fit may only result in a modest improvement in $R^2$ when the latter value approaches 100%. Thus, small differences in $R^2$ values across models should not be taken to mean that those models perform equally well, as performance analysis trades-off the sum-of-square residuals, not $R^2$, against number of model parameters.

## Performance analysis using Akaike's information criterion

We analyzed the performance of each model, that is, the goodness-of-fit relative to the number of parameters, using Akaike's information criterion (AIC) with sample-size correction ($AIC_C$). Although the AIC approach is certainly not new (Burnham & Anderson, 2002), only in relatively recent times has the method begun to be applied in certain scientific contexts, including visual neuroscience (e.g., Cornelissen, Wade, Vladusich, Dougherty, & Wandell, 2006; Elder & Sachs, 2004; Vladusich et al., 2006) and phylogenetics (Posada & Buckley, 2004). The core idea of the approach is to estimate the "loss of information" that occurs when one attempts to construct a model of reality. The measure of information loss consists of a mathematical term estimating the goodness-of-fit to a data set (e.g., sum-of-squares) and a term estimating the effect of the number of estimated parameters (i.e., complexity). In this sense, AIC embodies a statistical principle of parsimony.

Formally, we have

$$\mathrm{AIC}_C = N \ln\left(\frac{\mathrm{SS}_{\mathrm{fit}}}{N}\right) + 2K + \frac{2K(K+1)}{N-K-1}, \qquad (11)$$

where $N$ is the number of data points, $\mathrm{SS}_{\mathrm{fit}}$ is the fitted sum-of-squares, and $K$ is the number of fitted model parameters plus one (because the sum-of-squares is a "fitted parameter"). Generally speaking, the smaller the value of $\mathrm{AIC}_C$ the better the model has performed. By comparing $\mathrm{AIC}_C$ values for $i$th model to a comparison model (superscript $C$)

$$\Delta\mathrm{AIC}_c^i = \mathrm{AIC}_c^i - \mathrm{AIC}_c^C, \qquad (12)$$

we are able to rank the models ($r$) in the set ($R$). These $\Delta\mathrm{AIC}_C$ values are then exponentially transformed to compute the *relative probabilities $p_i$ of each model being correct*

$$p_i = \frac{e^{-0.5(\Delta\mathrm{AIC}_c^i)}}{\sum_r^R e^{-0.5(\Delta\mathrm{AIC}_c^r)}}. \qquad (13)$$

For comparison, we also compute a second criterion, known as the Bayesian information criterion (BIC),

$$\mathrm{BIC} = N \ln\left(\frac{\mathrm{SS}_{\mathrm{fit}}}{N}\right) + \ln(N). \qquad (14)$$

An analogous computation underlies the calculation of relative probabilities associated with the BIC method. A detailed discussion and comparison of the AIC and BIC approaches is provided in Burnham and Anderson (2002).

The general AIC approach has several advantages over tests conventionally used to compare models with different numbers of parameters (Burnham & Anderson, 2002). Of particular interest here, the AIC approach does not depend on arbitrary critical values for accepting or rejecting hypotheses and so does not require adjustments for multiple comparisons of the sort common to conventional statistical inference (e.g., Bonferroni correction). The AIC approach also allows one to compute evidence ratios with selected models (ratios of relative probabilities of each model being correct) or to add together the relative probabilities associated with specific models to examine the importance of parameters common to the selected models. We make particular use of these properties in our analysis. General discussions of the problems associated with conventional methods of statistical inference are provided elsewhere (Goodman, 1999a, 1999b; Sterne & Davey Smith, 2001). In common with conventional methods, the AIC approach depends on the assumption that model residuals are Gaussian-distributed with zero mean. We tested this assumption for all model fits using the D'Agostino–Pearson test for skewness and kurtosis, and the Students $t$ test for differences of the mean residuals from zero, respectively. We then considered whether the associated $R^2$ value and $p$ value together warranted strong evidence to exclude a given model from further analysis (see Table 1). In all cases where we excluded a model from the AIC hierarchy, had we allowed the model to be ranked, it would have been ranked last.

## Subjects

Eight subjects, four males and four females, with ages ranging from 21 to 41 and normal or corrected-to-normal vision, participated in the psychophysical experiment. Two subjects were experienced psychophysical observers who were aware of the experimental hypotheses, the others were naive observers, unaware of the hypotheses. None of the subjects reported having difficulty seeing in the dark, which might have indicated an increased sensitivity to ocular light scattering (stray light).

## Apparatus

Experiments were conducted in a darkened room on a calibrated computer monitor, an Eizo ColorEdge CG18 LCD (Eizo, Belgium) with 1,280 × 1,024 pixels native resolution and a 0.28-mm pixel dot. Using a GretagMacbeth Eye-One calibrator (GretagMacbeth, Switzerland), the maximum luminance of the LCD was set at 120 cd/m$^2$, the white point was set at 6,500 K and gamma for each primary channel was set at 2.2. Full colorimetric characterization of the display at these settings was performed using a Photo Research PR-650 spectrophotometer (Photo Research, Chatsworth, USA). We followed the characterization procedure as described by Cazes et al. (1999). Custom software for generating the stimuli ran on an Intel Pentium 4 computer with a 2.40-GHz processor and a graphics card with 8-bit color resolution per channel/gun. Our subjects were satisfied with the size of the luminance steps this set up allowed during achromatic color matching.

## Stimuli and tasks

Subjects dark adapted to the experimental room for several minutes. They then viewed stimuli at a distance of 0.72 m from the monitor. Stimuli consisted of a uniform background, which could have one of four luminance values (10, 40, 60, and 90 cd/m$^2$). To the left of the center of the screen (at 2.5° visual angle), the reference configuration consisted of a ring (subtending 2° visual angle) of constant luminance (50 cd/m$^2$) surrounding a 2° reference disk. The luminance of the reference disk varied between 29.9 and 83.3 cd/m$^2$ to produce 10 increments and 10 decrements relative to the ring. Ring-to-disk luminance ratios were evenly spaced on a log scale. An

| Model | AIC – BIC ranks | $R^2$ | $N$ | $K$ | AIC relative probability | BIC relative probability |
|---|---|---|---|---|---|---|
| Subject SWH | | | | | | |
| NOG | 4–4 | 97.01 | 40 | 5 | <.01 | <.01 |
| SAP | 2–2 | 98.68 | 40 | 6 | .4 | .41 |
| OPP | 5–5 | 97.03 | 40 | 6 | <.01 | <.01 |
| SIG | 1–1 | 98.70 | 40 | 6 | .49 | .51 |
| UP | 3–3 | 98.70 | 40 | 7 | .11 | .08 |
| Subject YIO | | | | | | |
| NOG* | 4–4 | 98.56 | 40 | 5 | <.01 | <.01 |
| SAP | 1–1 | 99.42 | 40 | 6 | .60 | .68 |
| OPP | 5–5 | 98.59 | 40 | 6 | <.01 | <.01 |
| SIG | 3–3 | 99.19 | 40 | 6 | <.01 | <.01 |
| UP | 2–2 | 99.45 | 40 | 7 | .40 | .31 |
| Subject LY | | | | | | |
| NOG | 4–4 | 97.83 | 40 | 5 | .09 | .14 |
| SAP | 1–1 | 98.12 | 40 | 6 | .41 | .36 |
| OPP** | 5–5 | 97.83 | 40 | 6 | .03 | .02 |
| SIG | 2–2 | 98.11 | 40 | 6 | .37 | .40 |
| UP** | 3–3 | 98.12 | 40 | 7 | .10 | .07 |

Table 1. Summary statistics for all models and subjects in Hong and Shevell (2004b). For subject SWH, the best-performing model was the SIG model followed by the SAP model. For subject YIO, the SAP model performed best, followed by the UP model. For subject LY, the evidence does not strongly favor any model. All relative probabilities are rounded up and so may not add exactly to 1. *Model residuals Gaussian-distributed but with nonzero mean ($p$ = .043). We included the model fit in the analysis because the mean was only just significantly different from zero. **Model did not converge within 250 iterations but $R^2$ value remained stable to two decimals points above 50 iterations. Note: $K$ = number of model parameters plus one (i.e., the sum-of-squares is an estimated parameter).

adjustable matching disk with the same angular size as the reference disk was placed to the right of the center of the screen (at 2.5° visual angle). The centers of the reference and matching disks were thus 5° apart. We used 2° disks and ring sizes to ensure maximum compatibility with the 2° luminosity function.

Subjects performed two tasks. They first set the luminance of the matching disk (initially 50 cd/m$^2$) such that the achromatic color of the matching disk appeared as similar as possible to the reference disk. We were very explicit in our instructions that subjects should match the achromatic color that they saw rather than the estimated albedo or lightness of the reference disk. After setting the match, subjects then rated (on a scale from 1 to 10) the relative ease with which the match was obtained. Subjects practiced these tasks on a trial set of stimuli before the experiment began. The experimental session lasted approximately 1 h, during which subjects could pause between trials. The entire experiment consisted of 80 unique combinations of background and reference disk luminance values. The order in which the four background conditions were presented to each subject was varied using a Latin square design to average out sequential effects. Within each background condition, trials were randomized, but decrements and increments were alternated to prevent possible effects of long-term contrast adaptation.

## Models of the new experimental data

For the psychophysical experiment performed here, we modeled the data with the following expression, based on Equation 3

$$\begin{aligned}\log T_m = {} & \log\frac{T_r C_m}{C_r} \\ & + w_{\mathrm{DB}}^{\mathrm{B}}\left[\log\frac{C_r}{NC_r}\right]^{+}\left(1-g_{\mathrm{B}}^{\mathrm{B}}\left[\log\frac{T_r}{C_r}\right]^{+}\right) \\ & \times\left(1-g_{\mathrm{D}}^{\mathrm{B}}\left[\log\frac{C_r}{T_r}\right]^{+}\right)-w_{\mathrm{DB}}^{\mathrm{D}}\left[\log\frac{NC_r}{C_r}\right]^{+} \\ & \times\left(1-g_{\mathrm{D}}^{\mathrm{B}}\left[\log\frac{T_r}{C_r}\right]^{+}\right)\left(1-g_{\mathrm{D}}^{\mathrm{D}}\left[\log\frac{C_r}{T_r}\right]^{+}\right), \quad (15)\end{aligned}$$

where the weights $w_{\mathrm{DB}}^{\mathrm{D}} \in \{w_{\mathrm{D}}^{\mathrm{D}}, w_{\mathrm{B}}^{\mathrm{D}}\}$ and $w_{\mathrm{DB}}^{\mathrm{B}} \in \{w_{\mathrm{D}}^{\mathrm{B}}, w_{\mathrm{B}}^{\mathrm{B}}\}$. The weights therefore depend on whether subjects make increment or decrement matches on the matching side of the display. This model is conceptually identical to the UP model used in the simulations of the Hong–Shevell data, expanded to include all possible polarity interactions

between local and remote increments and decrements in the reference display (8 free parameters). Strictly speaking, cross-polarity matches (matching local increments to decrements and vice versa) require a slight modification to the model because the local edge signals in matching and reference displays are no longer of the same polarity. This modification expands the total set of free parameters by four, but we found no improvements in performance. We therefore present the results obtained with the form of the UP model defined above.

We also implemented a more complex version of the UP model in which gain parameters were free to vary with the contrast of the remote edge

$$\log T_m = \log\frac{T_r C_m}{C_r} + w_{\mathrm{DB}}^{\mathrm{B}}\left[\log\frac{C_r}{NC_r}\right]^+ \times\left(1-g_{\mathrm{B}}^{\mathrm{B}C}\left[\log\frac{T_r}{C_r}\right]^+\right)\left(1-g_{\mathrm{D}}^{\mathrm{B}C}\left[\log\frac{C_r}{T_r}\right]^+\right) - w_{\mathrm{DB}}^{\mathrm{D}}\left[\log\frac{NC_r}{C_r}\right]^+\left(1-g_{\mathrm{D}}^{\mathrm{B}C}\left[\log\frac{T_r}{C_r}\right]^+\right) \times\left(1-g_{\mathrm{D}}^{\mathrm{D}C}\left[\log\frac{C_r}{T_r}\right]^+\right), \quad (16)$$

where the scripting of the gain parameters is generically defined as $g_j^{iC} \in \{g_j^{i\mathrm{H}}, g_j^{i\mathrm{L}}\}$, meaning that gain varied with the contrast (H = high, L = low) of the remote edge.

# Results

## Modeling of Hong–Shevell distance-dependent matching data

We first conducted simulations of the Hong and Shevell (2004b) experiments, wherein the position and polarity of the remote edge were manipulated. As indicated previously, Hong and Shevell (2004b) showed that the spatial extent of edge integration was greater for decrements of the remote edge than for increments. The present analysis focuses on evidence for gain control and as such forms a complementary line of inquiry to that undertaken in Hong and Shevell (2004b). We present only the data and fits for the condition in which the remote edge induced darkness into the target ring because this condition most clearly illustrates the contribution of gain control to matching behavior. One should keep in mind, however, that the UP model always generated the best fit because it had the largest number of parameters.

Figure 3 displays the fits obtained using the NOG, SIG, and SAP models for all subjects in that study. Although the fits associated with the three selected models appear quite similar at first glance, closer inspection reveals important differences. In particular, the blue lines (model predictions) do not coincide with the row of circular data points for the NOG model (Figure 3A), but the SIG and SAP models provide good fits for these points. The difference between the model fits illustrates the influence of gain control in the experiment. Although the effect is relatively robust, it is apparent that only detailed quantitative analysis could reveal gain control in this instance. Gain control is most obvious in the case of the blue curve because the local edge contrast is higher in this condition than in the others, meaning that blocking of the remote edge signal by the local edge has a greater influence.

Table 1 displays the information associated with each model for each subject. The table also ranks the models according to their calculated AIC and BIC scores and gives the relative probabilities of each ranked model being correct relative to the other ranked models. The results of the AIC and BIC methods agreed closely, providing strong evidence against the hypothesis of the NOG and the OPP models. The latter model always performed the worst, being ranked last for all subjects. Furthermore, the relative probabilities of this model being correct were always very low. In no case did unequivocal and unanimous evidence emerge to exclude any of the three remaining models, however.

Fitted parameter values for all simulations below are reported in Appendix. Here we discuss only the results obtained with the UP model because these parameter values are fairly representative. Inspection of the parameters for subject TG reveals that the fitted brightness gain parameter, with 95% confidence intervals ($g_{\mathrm{D}}^{\mathrm{B}} = 2.55 \pm 0.11$), is close to the value of the fitted darkness gain parameter ($g_{\mathrm{D}}^{\mathrm{D}} = 2.26 \pm 0.28$). This finding implies that gain control occurred equally for brightness and darkness, explaining why the SIG model was ranked first: the data do not strongly demand that brightness and darkness gain parameters be very different. For subject YIO, the evidence was more strongly in favor of the SAP and UP models (total relative AIC probability = 0.999). The poorer performance of the SIG model is evident from the fact that brightness and darkness gain parameters in the UP model were fit to very different values ($g_{\mathrm{D}}^{\mathrm{D}} = 4.72 \pm 0.19$, $g_{\mathrm{D}}^{\mathrm{B}} = 2.18 \pm 0.17$). In the case of subject LY, where the evidence does not strongly favor any one model of the three top-ranked models, inspection of the gain parameters associated with the UP model reveals a major discrepancy ($g_{\mathrm{D}}^{\mathrm{D}} = 1.71 \pm 0.33$, $g_{\mathrm{D}}^{\mathrm{B}} = -54.58 \pm 0$). Namely, the brightness gain parameter is negative. This observation is inconsistent with the blocking interpretation because it implies that the postgain induction signal must be larger than the pregain signal (see Methods). Given the relatively good performance of the competing models with positive

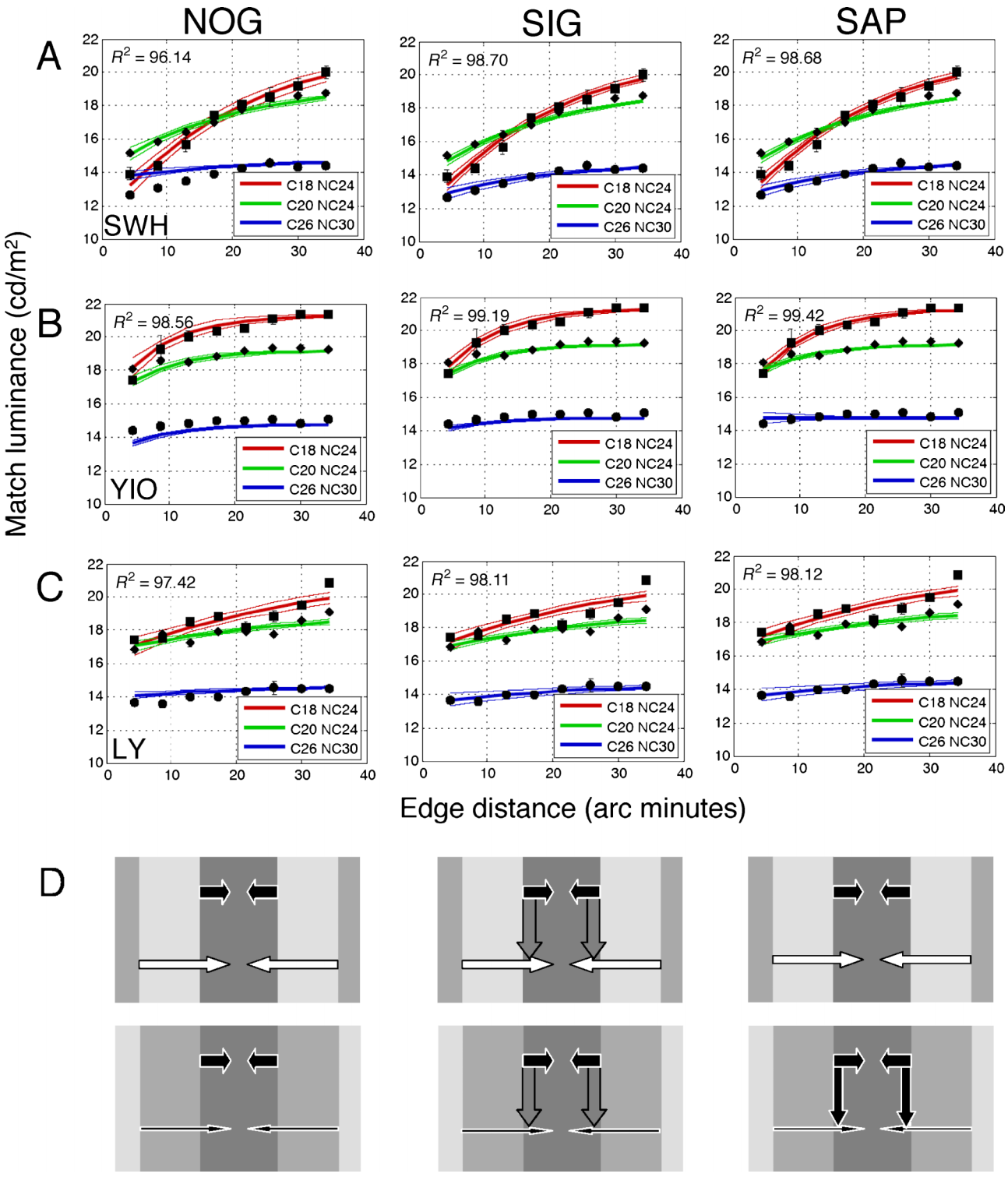


Figure 3. (A–C) Fits and 95% confidence intervals derived using the NOG, SIG, and SAP models for all subjects in Hong and Shevell (2004b). Hong and Shevell showed that the influence of the remote edge declines more slowly for increments than for decrements. For simplicity, here we plot the fits associated with decrements only. Differently colored lines and differently shaped symbols represent the different combinations of contiguous (C) and noncontiguous edges (NC) used in Hong and Shevell (2004b). For all subjects, the two gain control models shown above (as well as the UP model, fits not shown) provide better fits than the NOG model. Although these models contain one more parameter than the NOG model, the extra variance explained by the addition of the gain control parameters is justified in terms of the AIC and BIC performance analyses (see Table 1). (D) Schematic illustrations of the models.

or zero gain parameters, however, it would seem premature to conclude that the blocking interpretation is incorrect.

In summary, the present simulations reveal a previously hidden gain control effect in the data of Hong and Shevell (2004b). Our analysis also suggests a good deal of inter-subject variability with respect to the polarity specificity of this effect.

## Modeling of Hong–Shevell inverted-U function

We further studied the gain control models in simulations of the Hong and Shevell (2004a) experiments. These experiments demonstrated that darkness is related to the magnitude of the non-contiguous-inducing edge by an inverted-U-shaped function, provided that the local edge and remote edges both induce darkness. No such non-monotonicity arose when the local edge induced darkness and the remote edge induced brightness, or in control conditions where the contiguous and noncontiguous rings were replaced by a single solid ring. As shown in Figure 4, model fits were not as impressive as with the previous simulations: the $R^2$ value was higher than 95% for only one of the three subjects (TG), in the case of the best-fitting (UP) model. One of the remaining subjects (BS) generated a reasonable fit (~90%), whereas the fit for subject SWH was relatively poor (~70%). Table 2 displays all the statistics for this simulation.

Perhaps the most striking feature of Figure 4 is the failure of the NOG model to predict the inverted-U function for decrement–decrement edge combinations. The gain control (SIG and SAP) models, by comparison, are successful in various degrees in generating the inverted-U shape (Figure 4). In the following explanation, we adopt the expediency of dropping HWR brackets, inverting all negatively signed terms, and referring to the local darkness induction term as $\log\frac{T_r C_m}{C_r}$.

Three factors determine the shape of the matching function for these data points (assuming the SAP model). First, the local darkness induction term decreases as the luminance of the contiguous ring (18 – 22 cd/m$^2$) increases above the luminance of the target ring (16 cd/m$^2$). Alone, this would predict that subjects set matching luminance as a decreasing function of contiguous ring luminance (Figure 5A).

Second, the unblocked remote edge signal (Figure 5B), $w_D^D \log\frac{C_r}{NC_r}$, increases as contiguous ring luminance approaches noncontiguous ring luminance (24 cd/m$^2$). Third, the gain factor, $1 - g_D^D \log\frac{T_r}{C_r}$, decreases with increasing contiguous ring luminance. The multiplication of gain and remote induction signals with opposite slope thereby generates a nonlinearity (Figure 5B). The blocked remote induction signal then subtracts from the local induction term to generate the final matching function.

As with the previous simulations, individual subjects displayed some diversity in the best-performing models (Table 2). For subjects TG and BS, the SAP model was ranked first by the AIC method, closely followed by the UP model. The other models performed much worse. Interestingly, the story was a little different for subject SWH: the SIG model was ranked first, although the advantage over the other models was marginal. It is of interest to note that the SIG model was also AIC-ranked first for this subject in our simulations of the Hong and Shevell (2004b) study. We therefore have converging evidence that the SIG model may be the best model for this subject. Another interesting outcome is that, for subject SWH, the brightness weighting parameter in the UP model was negative ($w_D^B = -0.91 \pm 0.73$). This result agrees with our modeling of the Hong and Shevell (2004b) study above, suggesting that, in the special case of this subject, increments and decrements of the remote edge both trigger induction of surface darkness. For the other subjects, the values of the weighting parameters were consistent with the expected relationship between edge polarity and brightness or darkness (see Appendix).

Examination of the fitted values of the gain parameters for the remaining subjects reveals one important aberration. For subject BS, the brightness gain parameter in the UP model was negative ($g_D^B = -259.4 \pm 0.7$) although the darkness parameter was positive ($g_D^D = 8.4 \pm 0.2$). The negative value for the brightness parameter is inconsistent with the blocking interpretation. We found no parameter discrepancies for the remaining subjects.

To summarize, the present simulations quantify the gain control effects described qualitatively in Hong and Shevell (2004a), confirming that these data are consistent with a blocking interpretation. As with our simulations of the Hong and Shevell (2004b) data, the results provide strong evidence in favor of blocking between same-polarity edges and weaker evidence for blocking between opposite-polarity edges.

## An alternative gain control model

We studied a number of models in the course of our research. We do not present the complete set of results here because this would detract from the main themes of our study. One should keep in mind, however, that the non-monotonic-matching functions reported by Hong and Shevell (2004a) would be difficult to explain without recourse to some form of nonlinear gain control. We have been unable to generate nonmonotonicity, for instance, in a model in which monotonic responses to local and mean luminance form the basis of achromatic color percepts (Vladusich et al., 2006). Indeed, we have yet to find a situation in which nonmonotonicity arises in a model that is not based on edge integration theory.

We have, however, implemented a useful gain control model, based on edge integration theory, which cannot be conceptualized in terms of a blocking process (Equation 9). In this model, the remote edge controls the gain of the local edge, rather than the other way around. We found that the unconstrained version of this model performed comparably to the unconstrained (UP) blocking model.

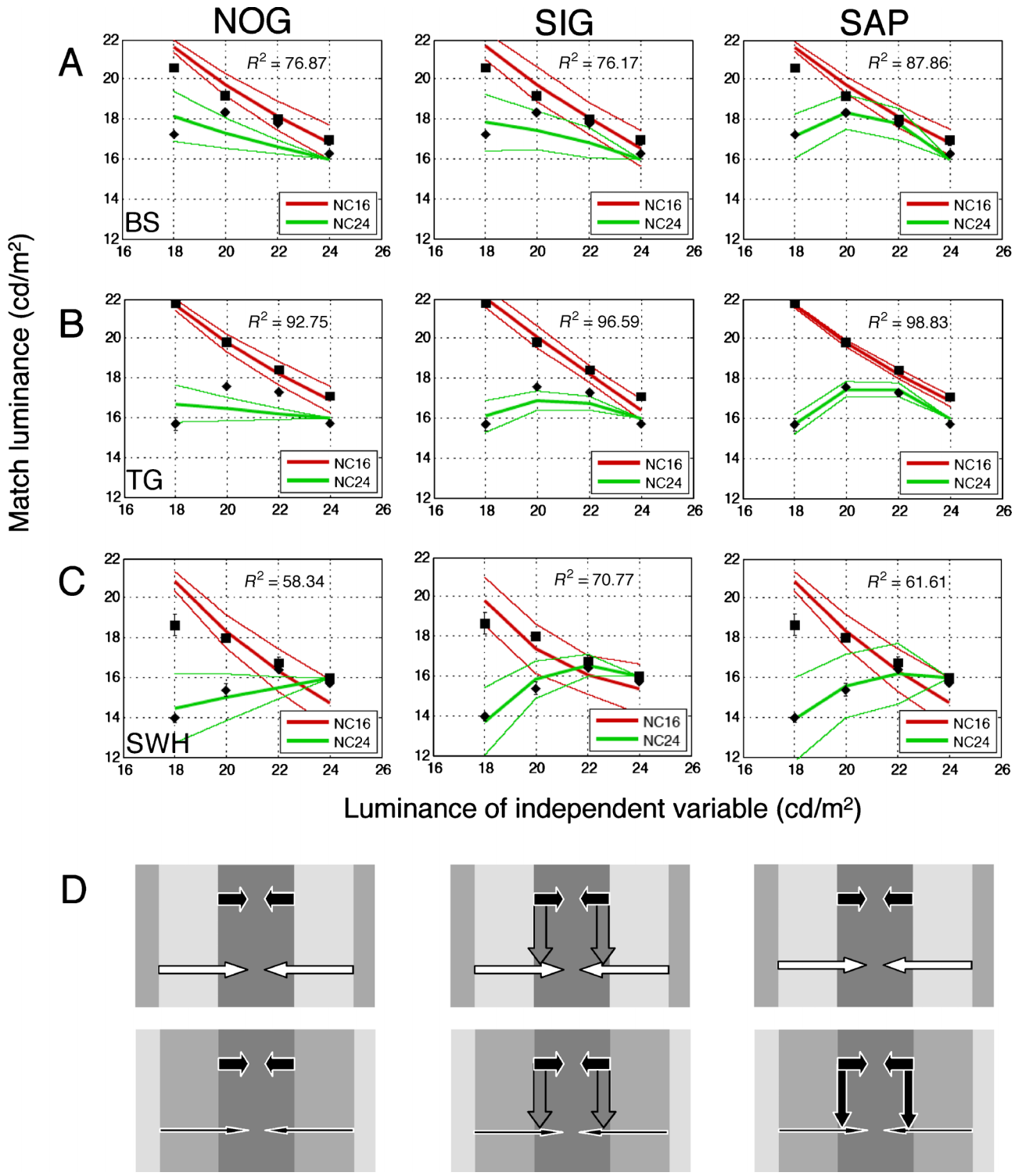


Figure 4. (A–C) Fits and 95% confidence intervals derived using the NOG, SIG, and SAP models for all three subjects in Hong and Shevell (2004b). Panels correspond to conditions where the local edge varied in luminance whereas the remote edge was kept constant at either 16 cd/m$^2$ (green lines and square data points) or 24 cd/m$^2$ (green lines and diamond data points). For simplicity, we do not show the results for conditions in which the local edge was kept constant and the remote edge varied or when the contiguous surface formed a solid region (without rings) extending to the edge of the background. The nonmonotonic functions (green) represent the psychophysical signature of the gain control process. For the subjects TG and BS, the SAP model performed the best (see Table 2 for performance indices). For subject SWH, the SIG model performed the best. We therefore find strong evidence for gain control in all subjects, albeit with no consensus concerning the specific form of the best-performing gain model. (D) Schematic illustrations of the models.

| Model | AIC – BIC ranks | $R^2$ | $N$ | $K$ | AIC relative probability | BIC relative probability |
|---|---|---|---|---|---|---|
| Subject BS | | | | | | |
| NOG | 3–3 | 76.87 | 16 | 3 | .02 | <.01 |
| SAP | 1–2 | 87.86 | 16 | 4 | .49 | .32 |
| OPP | 4–4 | 79.75 | 16 | 4 | <.01 | <.01 |
| SIG | 5–5 | 78.17 | 16 | 4 | <.01 | <.01 |
| UP* | 2–1 | 90.73 | 16 | 5 | .48 | .66 |
| Subject TG | | | | | | |
| NOG | 4–4 | 92.75 | 16 | 3 | <.01 | <.01 |
| SAP | 1–1 | 98.83 | 16 | 4 | .86 | .74 |
| OPP | 3–5 | 92.80 | 16 | 4 | <.01 | <.01 |
| SIG | 5–3 | 96.59 | 16 | 4 | <.01 | <.01 |
| UP | 2–2 | 98.88 | 16 | 5 | .14 | .26 |
| Subject SWH | | | | | | |
| NOG | 3–4 | 58.34 | 16 | 3 | .17 | .11 |
| SAP | 5–5 | 61.61 | 16 | 4 | .05 | .05 |
| OPP | 2–2 | 68.17 | 16 | 4 | .24 | .23 |
| SIG | 1–1 | 70.77 | 16 | 4 | .47 | .46 |
| UP | 4–2 | 71.45 | 16 | 5 | .06 | .14 |

Table 2. Summary statistics for all models and subjects in Hong and Shevell (2004a). For subjects BS and TG, the best-performing model was the SAP model closely followed by the UP model. For subject SWH, the SIG model performed best, as it did for this subject in our simulation of the Hong and Shevell (2004b) experiment. *Model did not converge within 250 iterations: $R^2$ value improved by ~.05 relative to 50 iterations.

The alternative model failed on a crucial test of validity, however, because the brightness weighting parameter was found to be positive for most subjects in the Hong–Shevell studies, implying that increments of the remote edge induce darkness, not brightness. Constraining the brightness weighting parameter to zero produced poor results. Because the alternative model did not produce realistic parameter values, we conclude that the blocking class of models provide a better account of the available data. In summary, we have not yet found an alternative model

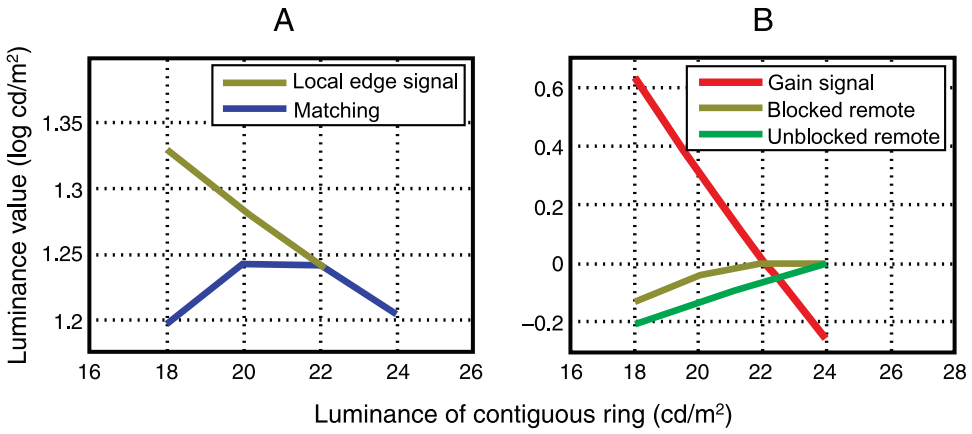


Figure 5. Illustration of how local and remote edge signals combine during blocking to generate an inverted-U-matching function with increasing contiguous ring luminance (note the different ordinate scales). The figure is based on the SAP model of subject TG's data. The luminance values for each model component are shown in log space on the ordinate. Local (A, dark yellow) and unblocked remote induction signals (B, dark yellow), as well as the gain or blocking signal (red), all change approximately linearly with increasing ring luminance. The multiplication of gain and unblocked remote-induction signals generates a nonlinearity in the blocked remote-induction signal. This signal is subtracted from the local induction signal, which is equivalent to division in linear space followed by a log transformation. The net effect is an inverted-U-shaped matching function.

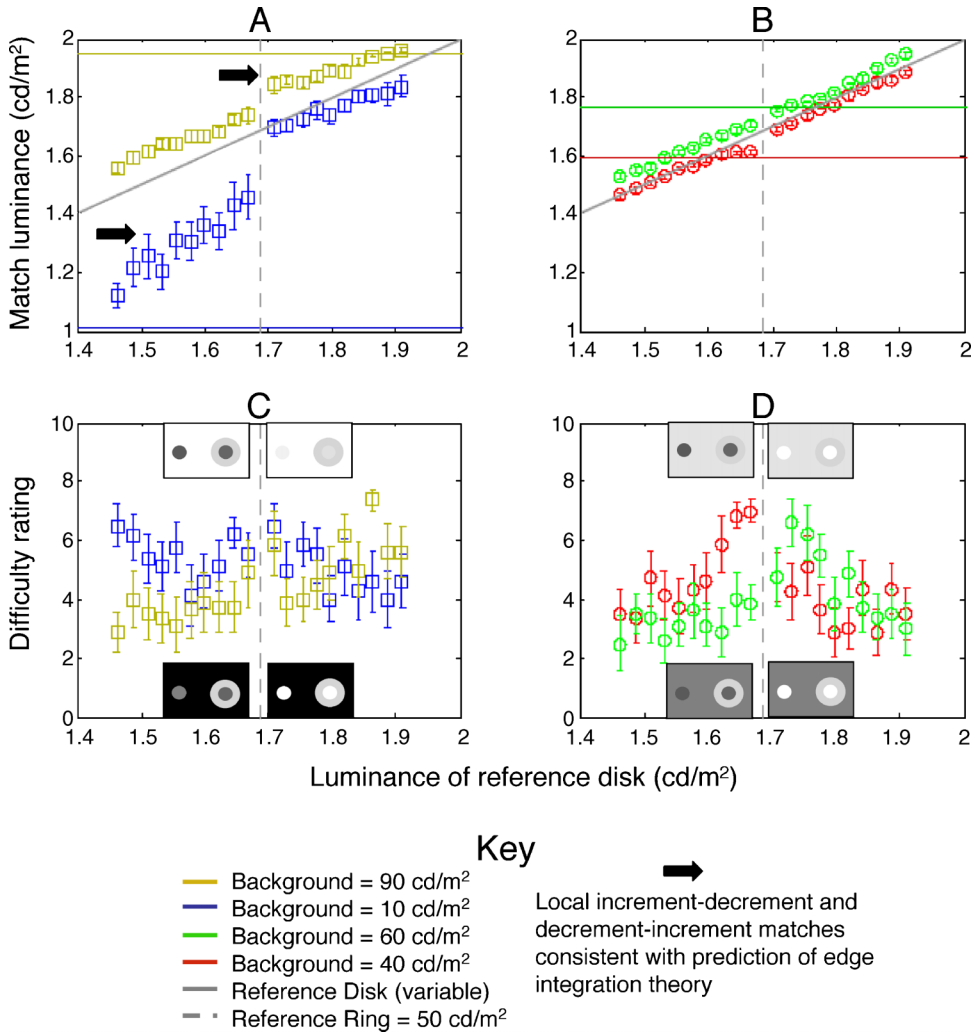


Figure 6. Results of the experimental test of edge integration theory, plotted on a log-log scale. The theory predicts that subjects should match local increments to decrements and vice versa when remote edge contrast is high. The two lower panels show the means and standard error of eight subjects, each making one setting per condition. As predicted, when the background luminance was very high or low (A), generating a high contrast at the remote edge, subjects made matches in accord with the polarity of the remote edge rather than the local edge. Subjects were far less inclined to set such increment–decrement (decrement–increment) matches when the background luminance values were less extreme and so remote edge contrast was relatively low (B). Subjects had more difficulty (C and D) making settings for opposite-polarity parings of local and remote edges than for same-polarity pairings when matches approached the luminance of the background.

which fits the Hong–Shevell data well and produces physically meaningful parameter values.

## An experimental test of edge integration theory

We conducted an achromatic color-matching experiment to test the prediction of edge integration theory that subjects should match local increments to decrements and vice versa in cases where the remote edge has high contrast and the opposite polarity relative to the local edge. Subjects set the luminance of a matching disk on a common background such that its achromatic color matched the achromatic color of a reference disk surrounded by a ring. We systematically varied the luminance of both the background and the reference disk, while keeping the luminance of the ring constant. Subjects also rated the difficulty of making each match to test the assumption that matches involving opposite-polarity edge combinations are as easy to make as matches involving same-polarity edge combinations.

The matching data support the prediction of edge integration theory (Figure 6). That is, subjects matched local increments to decrements and vice versa when the remote edge was of opposite polarity and high contrast relative to the local edge (Figure 6A). Subjects were far less inclined to set such cross-polarity matches when remote contrast was relatively low (Figure 6B). Moreover,

subjects never set cross-polarity matches when local and remote edges shared the same polarity. One might argue that subjects set cross-polarity matches because they had no alternative, given that the background luminance was so extreme in these instances. Such an explanation would not, however, take into account the linear relationship between matching and reference disk luminance. If subjects simply could not generate the appropriate achromatic colors in the matching disk, one would expect them to always set the luminance of the matching disk to the background luminance (because that is the closest option to the correct polarity relationship between local matching and reference edges). The linear relationship between matching and reference luminance shows that, although local edge contrast had a strong effect on achromatic color, the effect of the remote edge was more powerful, as predicted by edge integration theory.

The largest effects on matching luminance occurred in the case of decrement–increment combinations with the background luminance at 10 cd/m$^2$ (blue squares in the lower left quadrant of Figure 6A). These points showed the largest deviations from the grey line indicating the luminance of the reference disk and the greatest between-subject variance. Subjects also adopted a wide range of strategies in setting these cross-polarity matches (Supplementary material).

The rating data partially support the supposition that cross-polarity matches are more difficult to set than same-polarity matches, particularly when luminance settings approached the background luminance (Figures 6C and D). On top of this effect, subjects generally found matches difficult to make at low local edge contrasts. We speculate that this latter effect is due to the impression of transparency and fogginess in the reference disk at low contrasts (Ekroll, Faul, & Niederee, 2004). Our main interest here concerns whether opposite polarity combinations are more difficult to match than same-polarity combinations. We conducted paired $t$ tests on opposite- and same-polarity matches (pooled across background luminance values) separately for increments and decrements of the local edge. For decrements of the local edge, opposite-polarity combinations (mean difficulty rating = 5.14) were significantly harder ($p \ll .001$) to match than same-polarity combinations (mean difficulty rating = 3.47). We found no such difference for increments of the local edge ($p = .58$). This discrepancy may have arisen because the remote edge contrast associated with decrement–increment combinations of local and remote edges (50/10 cd/m$^2$) was higher than that associated with increment–decrement combinations (50/90 cd/m$^2$), leading to greater conflict between contrast and assimilation effects.

## Modeling the new matching data

We fit our data using the UP model defined in Equation 15 to investigate the nature of gain control in this experiment. To be consistent with blocking, model-matching functions should have slopes *less than one*. Visually, this implies that model-matching functions should be flatter than the grey line representing the luminance of the reference disk. We find that the fit of the model ($SS_{fit} = 258$) is reasonable for extreme values of the background luminance, or equivalently, high remote edge contrasts, but is far from perfect for the lower remote edge contrasts (Figure 7). In these cases, the model underestimates the amount of gain control evident in the data (the model-matching functions being close to unity).

To investigate gain control with greater fidelity, we modified the UP model to allow gain parameters to vary freely with remote edge contrast (Equation 16). This modification improved the fit by a factor of two ($SS_{fit} = 125$). According to both the AIC and BIC methods, the modified model outperformed the standard UP model substantially (relative $p = 1$ in favor of the modified model). The improvement is visually evident for both same and opposite-polarity combinations of local and remote edges, indicating that the failure of the standard UP model is not specifically related to the cross-polarity-matching issue.

We also found that gain control was often quantitatively different for same- and opposite-polarity pairings. In the case of same-polarity combinations, gain control parameters were always positive ($g_B^{BH} = 0.40 \pm 0.13$, $g_B^{BL} = 1.18 \pm 0.42$, $g_D^{DL} = 4.35 \pm 1.26$, $g_D^{DH} = 0.92 \pm 059$), consistent with blocking. With opposite-polarity combinations, gain control parameters were generally negative ($g_B^{DL} = -2.22 \pm 1.4$, $g_D^{BL} = -1.21 \pm 1.1$, $g_D^{DL} = -2.73 \pm 0.78$), consistent with "antiblocking" (Rudd & Popa, 2004a, 2004b). One exception occurred for decrement–increment combinations involving low remote edge contrast, where gain control was consistent with blocking ($g_B^{DH} = 0.86 \pm 0.55$).

We also modeled the data of individual subjects using the modified UP model (see Supplementary material for fits and performance indices). These findings confirm and extend the conclusions drawn above. We find strong effects of remote edge contrast on gain control parameters for various combinations of local and remote edge polarity (Figure 8). Decrement–increment combinations, on the one hand, are associated with antiblocking when remote edge contrast is *low,* consistent with our modeling of the mean data. Increment–decrement combinations, on the other hand, are associated with stronger antiblocking when remote edge contrast is *high,* again consistent with the mean data. Decrement–decrement and increment–increment combinations are both associated with stronger blocking when remote edge contrast is high. Although the prevalence of antiblocking at low contrast may be partly explained by problems setting satisfactory matches for opposite-polarity combinations, such an explanation cannot account for the stronger blocking effects at high contrast with same-polarity combinations.

We recognize that our modification of the standard UP model is ad hoc. We therefore applied a range of physically

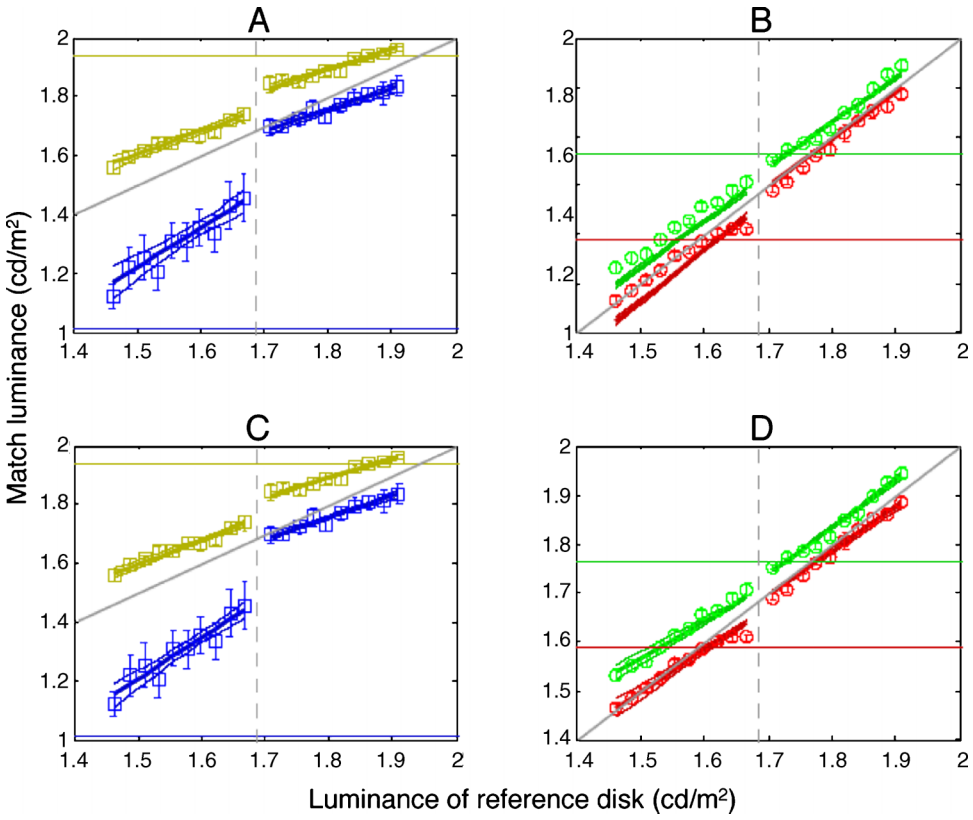


Figure 7. Modeling of the experimental test of edge integration theory (note different scales on left and right). The theory predicts that matching data can be fit with a single set of gain and weight factors for all background luminance values. (A–B) Fits generating under the assumption of a single set of gain parameters (UP model with parameters constrained for background luminance). (C–D) Fits generated under the assumption that gain parameters vary with background luminance (UP model with parameters unconstrained for background luminance). We find that the unconstrained model fits the data better and considerably outperforms the constrained model.

motivated modifications to the UP model, with little success. Additional study is clearly required to fully understand the nature of gain control in disk-ring displays.

## Discussion

Our work builds on several previous modeling studies aimed at understanding brightness and darkness perception (Land & McCann, 1971; Rudd & Arrington, 2001; Rudd & Zemach, 2004, 2005; Zaidi et al., 1992). Our modeling of the Hong and Shevell, (2004a, 2004b) data reveals robust gain control effects that can be interpreted as evidence for blocking in most cases (Rudd & Arrington, 2001). This conclusion is further reinforced by our modeling of achromatic color matching in the displays of Bressan and Actis-Grosso (2001), which appears as Supplementary material to this paper.

Our psychophysical and modeling results also suggest that claims concerning the polarity specificity of blocking need to be interpreted with caution (Rudd & Zemach, 2004). Displays containing local and remote edges of opposite polarity are sometimes associated with an apparent conflict between contrast and assimilation effects. This conflict may manifest itself in antiblocking. It also leads subjects to rate matches associated with opposite-polarity inducers as more difficult to set than those associated with inducers sharing the same polarity. A growing body of evidence indicates that perfect matches are not possible in situations where contrast and assimilation effects compete (Ekroll et al., 2004; Faul et al., 2006; Logvinenko & Maloney, 2006; Whittle, 1994). Precisely why subjects cannot always make satisfactory matches is an issue of ongoing research. Our discussion here focuses instead on clarifying the relationships among contrast, assimilation, and gain control effects.

### Relevance to understanding contrast and assimilation

To reiterate, edge integration theory predicts that the presence and magnitude of contrast and assimilation effects depends on the relative polarities and strengths of local and remote edge signals. One important factor in generating *net* assimilation effects—defined as cases in which subjects

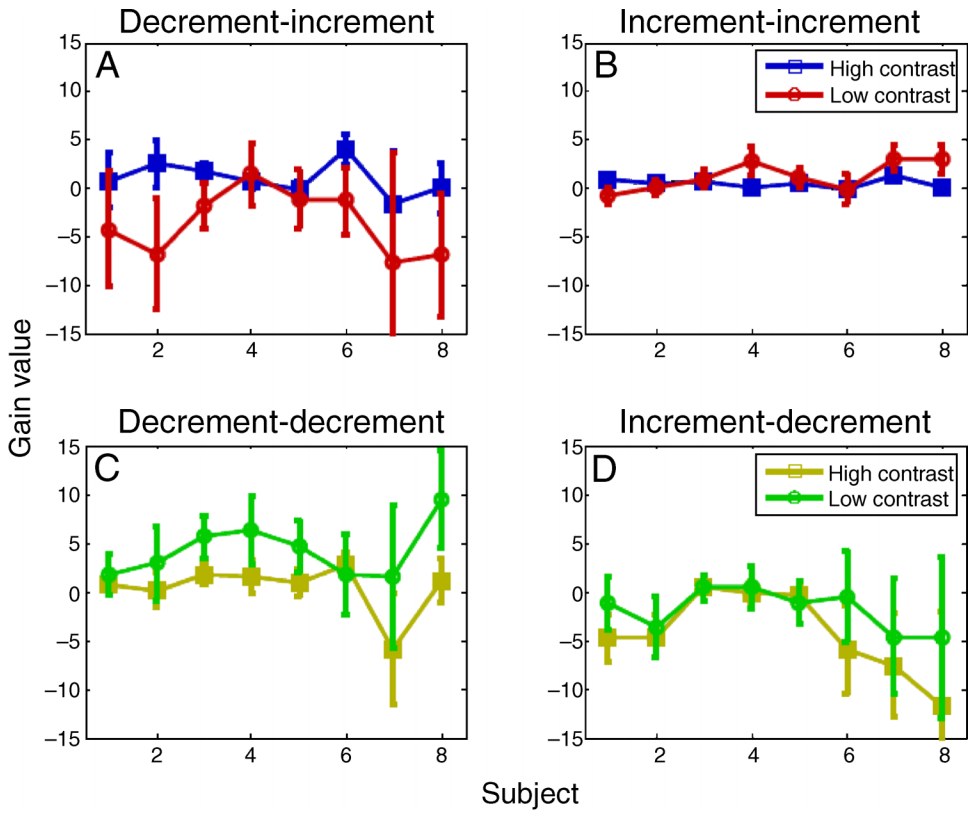


Figure 8. Fitted gain control parameters with 95% confidence intervals from modeling of individual subject's data using the unconstrained UP model (Supplementary material). Color coding corresponds to that used in earlier figures. (A) Fitted gain control parameters for low and high contrast values of the remote edge, with decrement–increment combinations of local-remote edges. Gain values at the low contrast are negative for most subjects, consistent with antiblocking. (B) Contrast had less effect for increment–increment combinations for most subjects. (C) For decrement–decrement combinations, however, the low contrast of the remote edge is associated with large positive gain control values, consistent with blocking. (D) The effect of contrast on gain is less clear for increment–decrement combinations.

match local increments to decrements and vice versa—is the physical polarity and contrast of the remote edge relative to the physical contrast of the local edge. When the two edges have opposite polarities and remote contrast is high and the local contrast low, assimilation may completely overshadow any perceptual contrast effect associated with the local edge. The magnitude of the assimilation effect will also depend on the value of the putative gain parameter.

Hong and Shevell (2004a) made the distinction among contrast, assimilation, and blocking effects in their matching data. Here we modeled these data within the context of edge integration theory. Although we find that the edge integration theory provides a good quantitative account of the data in most cases, we could not identify a single best blocking model for all subjects. This may mean that either the parameters underlying edge integration vary widely across subjects, that our simplifications of the stimulus conditions were more important than we had assumed, or that the theory is wrong or incomplete. All our attempts to find a better set of models to account for these data have failed, however. Our results therefore concur with the conclusions of Hong and Shevell (2004a) that achromatic color perception in circularly symmetric displays is well described by edge integration theory.

Our explanation of the nonmonotonic relation between darkness perception and contiguous ring luminance, however, differs from the interpretation of Hong and Shevell (2004a). These authors remarked on the role of assimilation in generating nonmonotonicity but did not state specifically how assimilation might relate to blocking. We instead claim that nonmonotonicity is due to blocking of a *contrast* effect induced from the remote edge, which shared the polarity of the local edge. This hypothesis can be tested by having subjects rate the difficulty of making matches made under conditions supporting either monotonic and nonmonotonic functions. We predict no difference in difficulty ratings when both types of functions are associated with (same-polarity) contrast effects.

Bindman and Chubb (2004) studied contrast and assimilation effects in bull's-eye patterns, which are essentially complicated versions of the stimuli studied here (see also Güçlü & Farell, 2005, pp. 1175–76). The authors reported dramatic differences between the strength of the assimilation effect with different tasks.

They measured a stronger assimilation effect using a two-alternative forced choice task than that obtained with an achromatic color-matching task. This discrepancy might be related to our findings that the conditions supporting assimilation—situations in which local and remote edges are of opposite polarity—are associated with a range of behaviors that one does not observe with stimuli evoking only contrast effects. In the mixed polarity case, our subjects showed greater variability in their settings, matched local increments to decrements and vice versa, and had greater difficulty in setting matches. The present findings therefore imply that the achromatic color-matching method is not a satisfactory means of assessing the strength of assimilation. Whether the forced choice paradigm veridically measures the strength of assimilation remains unclear.

## The nature of gain control

Rudd and Zemach (2004) rejected the blocking interpretation on the grounds that the data did not consistently favor a blocking interpretation in the four subjects tested. Data from two subjects supported the blocking interpretation, whereas the remaining subjects showed either no evidence for gain control or an antiblocking effect. Since Rudd and Zemach (2004) used stimuli in which local and remote edges had opposite polarities, their data are particularly relevant for our study.

Our analyses of the Hong–Shevell data generally support the conclusions of Rudd and Zemach (2004), suggesting that gain control interactions between edges of opposite polarity are associated with a great amount of variability across subjects. Our psychophysical data may shed light on this issue. We found large between-subject variability in matches made under conditions similar to those studied in Rudd and Zemach (2004): namely, when local and remote edges had opposite polarities and the local edge was a decrement. One important difference is that subjects in Rudd and Zemach (2004) never set increment–decrement matches. It is interesting to note, from this perspective, that the subject (JL) whose data were consistent with antiblocking came the closest to making increment–decrement matches. In our data, subjects often tended to set the luminance of the matching disk close to the background luminance when confronted with difficulty, thereby flattening out the matching function in the direction of antiblocking. Our modeling of individual subject's data (Supplementary material) reveals that antiblocking is most prominent when matches approach the background luminance. We are therefore unable to determine whether antiblocking is a genuine effect or a by-product of the inability of subjects to set satisfactory matches under these conditions.

It is interesting to note that the strongest assimilation effects reported in the forced choice task of Bindman and Chubb (2004) occurred when the local edge had the highest physical contrast. This finding is consistent with much of our matching data and with an antiblocking effect. Nevertheless, we suggest that future empirical studies of assimilation and gain control would benefit from avoiding the use of matching tasks. It seems likely that in such situations subjects are simply making the best of a bad situation (Ekroll et al., 2004).

We describe here an additional effect of gain control. We found that regardless of the polarity relationship between local and remote inducers, our matching data were better described by a model in which gain varied with the luminance of the background. We cannot distinguish on the basis of our results whether the effect arises from changes in the luminance of the background itself or from the accompanying changes in the contrast of the remote edge. Rudd and Popa (2004a, 2004b) have reported a similar change in the effect of gain control with the distance between local and remote inducers, suggesting the involvement of a feedback gain control process between nearby edges. Our results agree with their conclusions, suggesting that the direction and magnitude of feedback gain control (positive or negative) depends on the polarity and contrast of remote edges.

## Relevance to achromatic color filling-in

Edge integration theory (Rudd & Arrington, 2001) derives partly from retinex theory (Land & McCann, 1971) and partly from the filling-in theory of brightness and darkness perception (Cohen & Grossberg, 1984; Grossberg & Todorovic, 1988). According to the model of Grossberg and Todorovic (1988), the filling-in of brightness and darkness is blocked by edge signals that are not sensitive to polarity. Arrington (1996) modified this model, incorporating a directional filling-in mechanism that allows brightness (darkness) to flow across borders of the same polarity but not the opposite polarity. In the present context, Arrington's model predicts that blocking should occur *only between edges of opposite polarity*. The available evidence does not support this prediction.

In considering blocking in terms of filling-in, it is important to note that recent functional magnetic resonance imaging (fMRI) studies provide conflicting evidence concerning the existence of brightness and color filling-in in early visual cortex. On the one hand, the studies of Meng, Remus, and Tong (2005) and Sasaki and Watanabe (2004) provide evidence in favor of filling-in. On the other hand, Boucard, van Es, Maguire, and Cornelissen (2005), Cornelissen et al. (2006), and Perna, Tosetti, Montanaro, and Morrone (2005) report evidence against filling-in in V1 and V2. It is likely, however, that reports in favor of filling-in (Meng et al., 2005; Sasaki & Watanabe, 2004) may have contained real or illusory edge signals within the region of interest (Cornelissen et al., 2006; Cornelissen & Vladusich, in press). Modeling of neuronal V1 responses to stimuli similar to those studied here (Kinoshita & Komatsu, 2001)

also fails to support the filling-in hypothesis in most neurons (Vladusich et al., 2006). Filling-in may occur in higher cortical areas (Perna et al., 2005), or may not occur at all, with the latter possibility being consistent with the notion that surface brightness is coded by the activity of edge-sensitive neurons (Bindman & Chubb, 2004; Blakeslee & McCourt, 1999, 2004; Blakeslee et al., 2005; Friedman, Zhou, & von der Heydt, 2003; Rudd & Zemach, 2004; Zhou, Friedman, & von der Heydt, 2000).

## The neural basis of edge integration

The framework developed here generalizes the edge integration theory introduced in Rudd and Arrington (2001) to incorporate a neural mechanism for defining polarity-specific edge interactions. We should note, however, that Rudd and Zemach (2004) implicitly joined together the concepts of log luminance ratio processing and HWR processing in their discussion of how cortical simple cells might implement edge integration. The explicit union of HWR notation with log luminance ratios (Vladusich et al., 2006) provides a compact and physically motivated means of associating different weights and gains with edge signals of opposite polarity.

Parallel processing of local luminance increments and decrements occurs within ON and OFF channels of the retina and lateral geniculate nucleus (Bowen, 1997; Schiller, 1992). In the cortex, polarity-sensitive neurons, such as simple cells, are routinely modeled as HWR mechanisms that combine ON and OFF signals (Grossberg & Mingolla, 1985; Heeger, 1993). Simple cells may provide a neural basis for psychophysical effects related to edge detection (Elder & Sachs, 2004; Grossberg & Mingolla, 1985; Sankeralli & Mullen, 2001) and brightness coding (Bindman & Chubb, 2004; Blakeslee & McCourt, 1999, 2004; Blakeslee et al., 2005). Thus, simple cells are the most likely candidates to provide inputs to the putative edge integration process.

## Possible relevance to White's effect

Howe (2005) introduced a simplified variant of White's effect (White, 1979) using circularly symmetric displays, similar to those studied by Bindman and Chubb (2004) and Hong and Shevell (2004a, 2004b), containing multiple black and white rings, some of which were replaced by grey test rings. Howe (2005) employed a matching task to measure the strength of the illusion in conventional and simplified displays. He found that the illusion was not diminished in the simplification, implying that figural factors are not essential to the production of the effect. Here we present a simpler display—based on our experimental data and modeling work with edge integration theory—which may have important implications for White's effect (Figure 9). Our goal is to theoretically motivate further empirical study on the roles of contrast and assimilation in White's effect (Blakeslee et al., 2005; De Weert & Spillmann, 1995; Ripamonti & Gerbino, 2001; Spehar & Zaidi, 1997), rather than to provide an account of the phenomenon per se.

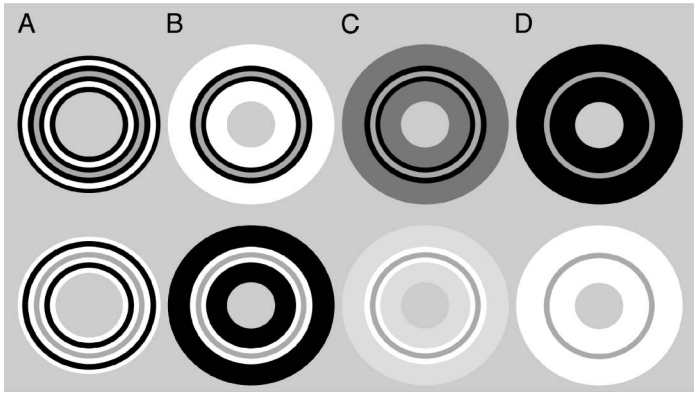


Figure 9. Displays based on our study of contrast and assimilation. (A) Display similar to the Howe (2005) version of White's effect. (B) Display which is further simplified from (A) suggests a link between the assimilation effects studied here, bull's-eye displays (Bindman & Chubb, 2004), and White's effect. The local edge formed by the grey ring and the contiguous ring induces a contrast effect directly into the grey ring, whereas the remote edge formed by the contiguous and noncontiguous rings induces an assimilation effect (we neglect the influence of the outermost edge for simplicity). (C) The assimilation effect is largely eliminated by reducing the contrast associated with the remote edge. (D) Conventional simultaneous contrast illusion. The display in (B) does not manifest strong figural grouping, making it potentially useful for isolating the role of assimilation in White's effect.

The displays in Figure 9 were designed to elicit competing contrast and assimilation effects. This was done by ensuring that local and remote edges have opposite polarities—a property necessary for the induction of White's effect (Spehar & Zaidi, 1997)—and that the remote edge has higher contrast than the local edge. These are precisely the conditions under which subjects set cross-polarity matches in our experiment. The local edge in Figures 9A and B induces a contrast effect into the grey central ring. The high physical contrast associated with the remote edge, however, ensures that assimilation is also induced into the target ring. Thus, although the local edge is weighted more highly than the remote edge by virtue of its proximity to the target region, the high contrast of the remote inducer partially overrides the contrast effect. In other words, it may be that a simple assimilation effect (Blakeslee et al., 2005; De Weert & Spillmann, 1995) can explain the circular variant—and perhaps at least a part of the effect observed in the conventional variant—of White's display (Ripamonti & Gerbino, 2001). Consistent with our matching data, the circular variant illustrated in Figure 9C shows that lowering the contrast associated with the remote edge largely eliminates any assimilation effect.

## Concluding remarks

We have shown that edge integration theory accounts for a wide variety of achromatic color-matching data. The theory also suggests a number of avenues for further empirical work. Of particular importance is to identify how conflict between contrast and assimilation effects may give rise to the difficulty subjects experience in setting achromatic color matches under certain conditions (Faul et al., 2006; Logvinenko & Maloney, 2006).

# Appendix A

| Model (rank) | $g_D^B$ | $g_D^D$ | $m_D^B$ | $m_D^D$ | $k_D^B$ | $k_D^D$ |
|---|---|---|---|---|---|---|
| | | | Subject SWH | | | |
| NOB (4) | – | | −0.03 ± 0.09 | 0.06 ± 0.01 | −0.06 ± 0.14 | 1.93 ± 0.21 |
| SAP (2) | 0 | 2.26 ± 0.28 | −0.03 ± 0.06 | 0.06 ± 0.01 | −0.06 ± 0.09 | 2.36 ± 0.17 |
| OPP (5) | 2.55 ± 0.16 | 0 | −0.03 ± 0.07 | 0.06 ± 0.01 | −0.19 ± 0.34 | 1.93 ± 0.21 |
| SIB (1) | 2.27 ± 0.28 | | −0.03 ± 0.05 | 0.06 ± 0.1 | −0.15 ± 0.2 | 2.36 ± 0.17 |
| UP (3) | 2.55 ± 0.11 | 2.26 ± 0.28 | −0.03 ± 0.05 | 0.06 ± 0.01 | −0.19 ± 0.23 | 2.36 ± 0.18 |
| | | | Subject YIO | | | |
| NOB (4) | – | | 0.07 ± 0.04 | 0.13 ± 0.04 | 0.75 ± 0.27 | 0.97 ± 0.29 |
| SAP (1) | 0 | 4.72 ± 0.19 | 0.07 ± 0.02 | 0.13 ± 0.02 | 0.75 ± 0.18 | 1.46 ± 0.25 |
| OPP (5) | 2.18 ± 0.27 | 0 | 0.07 ± 0.03 | 0.13 ± 0.04 | 1.75 ± 0.24 | 0.97 ± 0.29 |
| SIB (3) | 2.82 ± 0.22 | | 0.07 ± 0.03 | 0.13 ± 0.03 | 2.78 ± 0.14 | 1.25 ± 0.26 |
| UP (2) | 2.18 ± 0.17 | 4.72 ± 0.19 | 0.07 ± 0.02 | 0.13 ± 0.02 | 1.75 ± 0.15 | 1.46 ± 0.25 |
| | | | Subject LY | | | |
| NOB (4) | – | | 0.23 ± 0.18 | 0.04 ± 0.01 | 0.56 ± 0.25 | 0.86 ± 0.13 |
| SAP (1) | 0 | 1.71 ± 0.32 | 0.23 ± 0.17 | 0.04 ± 0.01 | 0.56 ± 0.24 | 0.98 ± 0.14 |
| OPP (5) | −54.58 ± 0 | 0 | 0.22 ± 0.35 | 0.04 ± 0.01 | 0.04 ± 0.07 | 0.86 ± 0.13 |
| SIB (2) | 1.67 ± 0.32 | | 0.23 ± 0.17 | 0.04 ± 0.01 | 1.01 ± 0.15 | 0.98 ± 0.14 |
| UP (3) | −54.58 ± 0 | 1.71 ± 0.33 | 0.22 ± 0.33 | 0.04 ± 0.01 | 0.04 ± 0.07 | 0.98 ± 0.15 |

Table A1. Fitted parameters and 95% confidence intervals for simulations of Hong and Shevell (2004b).

| Model (rank) | $g_D^B$ | $g_D^D$ | $w_D^B$ | $w_D^D$ |
|---|---|---|---|---|
| | | Subject BS | | |
| NOG (3) | – | | 0.13 ± 0.13 | 0.56 ± 0.23 |
| SAP (1) | – | 8.37 ± 0.43 | 0.13 ± 0.1 | 1.31 ± 0.35 |
| OPP (4) | −259.4 ± 0.1 | – | <0.01 ± 0 | 0.56 ± 0.23 |
| SIG (5) | 3.02 ± 0.39 | | 0.18 ± 0.23 | 0.73 ± 0.3 |
| UP (2) | −259.4 ± 0.7 | 8.37 ± 0.2 | <0.01 ± 0 | 1.31 ± 0.33 |
| | | Subject TG | | |
| NOG (4) | – | | 0.14 ± 0.1 | 0.85 ± 0.2 |
| SAP (1) | – | 7.15 ± 0.19 | 0.14 ± 0.04 | 1.67 ± 0.15 |
| OPP (5) | 2.01 ± 0.22 | – | 0.2 ± 0.14 | 0.85 ± 0.2 |
| SIG (3) | 4.65 ± 0.48 | | 0.37 ± 0.21 | 1.28 ± 0.21 |
| UP (2) | 2.01 ± 0.37 | 7.15 ± 0.13 | 0.2 ± 0.06 | 1.67 ± 0.15 |
| | | Subject SWH | | |
| NOG (3) | – | | −0.2 ± 0.2 | 1.35 ± 0.4 |
| SAP (5) | – | 3.97 ± 0.7 | −0.2 ± 0.2 | 1.87 ± 0.55 |
| OPP (2) | 5.2 ± 1.16 | – | −0.91 ± 0.72 | 1.35 ± 0.37 |
| SIG (1) | 5.04 ± 1.1 | | −0.86 ± 0.66 | 2.07 ± 0.57 |
| UP (4) | 5.2 ± 1.24 | 3.97 ± 0.59 | −0.91 ± 0.73 | 1.87 ± 0.5 |

Table A2. Fitted parameters and 95% confidence intervals for simulations of Hong and Shevell (2004a).

## Acknowledgments

This work was supported by grant 051.02.080 of the Cognition program of The Netherlands Organization for Scientific Research (NWO). We thank L. Tiggelaar for help in gathering data for the experiment.

Commercial relationships: none.
Corresponding author: Tony Vladusich.
E-mail: t.vladusich@med.umcg.nl.
Address: PO Box 300001, 9700 RB, Groningen, The Netherlands.

## References

Arrington, K. F. (1996). Directional filling-in. *Neural Computation, 8,* 300–318. [PubMed]

Beer, R. D., & MacLeod, D. I. (2000). Pre-exposure to contrast selectively compresses the achromatic half-axes of color space. *Vision Research, 40,* 3083–3088. [PubMed]

Bindman, D., & Chubb, C. (2004). Brightness assimilation in bullseye displays. *Vision Research, 44,* 309–319. [PubMed]

Blakeslee, B., & McCourt, M. E. (1999). A multiscale spatial filtering account of the White effect, simultaneous brightness contrast and grating induction. *Vision Research, 39,* 4361–4377. [PubMed]

Blakeslee, B., & McCourt, M. E. (2004). A unified theory of brightness contrast and assimilation incorporating oriented multiscale spatial filtering and contrast normalization. *Vision Research, 44,* 2483–2503. [PubMed]

Blakeslee, B., Pasieka, W., & McCourt, M. E. (2005). Oriented multiscale spatial filtering and contrast normalization: A parsimonious model of brightness induction in a continuum of stimuli including White, Howe and simultaneous brightness contrast. *Vision Research, 45,* 607–615. [PubMed]

Boucard, C. C., van Es, J. J., Maguire, R. P., & Cornelissen, F. W. (2005). Functional magnetic resonance imaging of brightness induction in the human visual cortex. *NeuroReport, 16,* 1335–1338. [PubMed]

Bowen, R. W. (1997). Isolation and interaction of ON and OFF pathways in human vision: Contrast discrimination at pattern offset. *Vision Research, 37,* 185–198. [PubMed]

Bressan, P., & Actis-Grosso, R. (2001). Simultaneous lightness contrast with double increments. *Perception, 30,* 889–897. [PubMed]

Burnham, K. P., & Anderson, D. R. (2002). *Model selection and multimodel inference: A practical information-theoretic approach*. New York: Springer.

Cazes, A., Braudaway, G., Christensen, J., Cordes, M. D., Lien, D., A., Mintzer, F., et al. (1999). On the color calibration of liquid crystal displays. *Proceedings of the SPIE Conference on Display Metrology, San Jose,* 154–161.

Cohen, M. A., & Grossberg, S. (1984). Neural dynamics of brightness perception: Features, boundaries, diffusion, and resonance. *Perception & Psychophysics, 36,* 428–456. [PubMed]

Cornelissen, F. W., & Vladusich, T. (in press). What gets filled-in during filling-in? *Nature Reviews Neuroscience*.

Cornelissen, F. W., Wade, A. R., Vladusich, T., Dougherty, R. F., & Wandell, B. A. (2006). No functional magnetic resonance imaging evidence for brightness and color filling-in in early human visual cortex. *The Journal of Neuroscience, 26,* 3634–3641. [PubMed]

De Weert, C. M., & Spillmann, L. (1995). Assimilation: Asymmetry between brightness and darkness? *Vision Research, 35,* 1413–1419. [PubMed]

Ekroll, V., Faul, F., & Niederee, R. (2004). The peculiar nature of simultaneous colour contrast in uniform surrounds. *Vision Research, 44,* 1765–1786. [PubMed]

Elder, J. H., & Sachs, A. J. (2004). Psychophysical receptive fields of edge detection mechanisms. *Vision Research, 44,* 795–813. [PubMed]

Faul, F., Ekroll, V., & Vladusich, T. (2006). Conditions for the impossibility of asymmetric brightness matching. Poster presented at Tagung Experimentell Arbeitender Psychologen, March 26–29, Mainz, Germany.

Friedman, H. S., Zhou, H., & von der Heydt, R. (2003). The coding of uniform colour figures in monkey visual cortex. *The Journal of Physiology, 548,* 593–613. [PubMed] [Article]

Goodman, S. N. (1999a). Toward evidence-based medical statistics: I. The *P* value fallacy. *Annals of Internal Medicine, 130,* 995–1004. [PubMed] [Article]

Goodman, S. N. (1999b). Toward evidence-based medical statistics: II. The Bayes factor. *Annals of Internal Medicine, 130,* 1005–1013. [PubMed] [Article]

Grossberg, S., & Mingolla, E. (1985). Neural dynamics of form perception: Boundary completion, illusory figures, and neon color spreading. *Psychological Review, 92,* 173–211. [PubMed]

Grossberg, S., & Todorovic, D. (1988). Neural dynamics of 1-D and 2-D brightness perception: A unified model of classical and recent phenomena. *Perception & Psychophysics, 43,* 241–277. [PubMed]

Güçlü, B., & Farell, B. (2005). Influence of target size and luminance on the White–Todorovic effect. *Vision Research, 45,* 1165–1176. [PubMed]

Heeger, D. J. (1993). Modeling simple-cell direction selectivity with normalized, half-squared, linear operators. *Journal of Neurophysiology, 70,* 1885–1898. [PubMed]

Helson, H. (1963). Studies of anomalous contrast and assimilation. *Journal of the Optical Society of America, 53,* 179–184. [PubMed]

Hong, S., & Shevell, S. K. (2004a). Brightness contrast and assimilation from patterned inducing backgrounds. *Vision Research, 44,* 35–43. [PubMed]

Hong, S. W., & Shevell, S. K. (2004b). Brightness induction: Unequal spatial integration with increments and decrements. *Visual Neuroscience, 21,* 353–357. [PubMed]

Howe, P. D. (2005). White's effect: Removing the junctions but preserving the strength of the illusion. *Perception, 34,* 557–564. [PubMed]

Kinoshita, M., & Komatsu, H. (2001). Neural representation of the luminance and brightness of a uniform surface in the macaque primary visual cortex. *Journal of Neurophysiology, 86,* 2559–2570. [PubMed] [Article]

Land, E. H., & McCann, J. J. (1971). Lightness and retinex theory. *Journal of the Optical Society of America, 61,* 1–11. [PubMed]

Logvinenko, A. D., & Maloney, L. T. (2006). The proximity structure of achromatic surface colors and the impossibility of asymmetric lightness matching. *Perception & Psychophysics, 68,* 76–83. [PubMed]

Meng, M., Remus, D. A., & Tong, F. (2005). Filling-in of visual phantoms in the human brain. *Nature Neuroscience, 8,* 1248–1254. [PubMed]

Perna, A., Tosetti, M., Montanaro, D., & Morrone, M. C. (2005). Neuronal mechanisms for illusory brightness perception in humans. *Neuron, 47,* 645–651. [PubMed]

Posada, D., & Buckley, T. R. (2004). Model selection and model averaging in phylogenetics: Advantages of Akaike information criterion and Bayesian approaches over likelihood ratio tests. *Systems Biology, 53,* 793–808. [PubMed]

Ripamonti, C., & Gerbino, W. (2001). Classical and inverted White's effects. *Perception, 30,* 467–488. [PubMed]

Rudd, M. E., & Arrington, K. F. (2001). Darkness filling-in: A neural model of darkness induction. *Vision Research, 41,* 3649–3662. [PubMed]

Rudd, M. E., & Popa, D. (2004a). A theory of the neural processes underlying edge integration in human lightness perception [Abstract]. *Journal of Vision, 4*(8), 345a, http://journalofvision.org/4/8/345/, doi:10.1167/4.8.345.

Rudd, M. E., & Popa, D. (2004b). Edge integration and edge interaction in achromatic color computation [Abstract]. *Journal of Vision, 4*(11), 79a, http://journalofvision.org/4/11/79/, doi:10.1167/4.11.79.

Rudd, M. E., & Zemach, I. K. (2004). Quantitative properties of achromatic color induction: An edge integration analysis. *Vision Research, 44,* 971–981. [PubMed]

Rudd, M. E., & Zemach, I. K. (2005). The highest luminance anchoring rule in achromatic color perception: Some counterexamples and an alternative theory. *Journal of Vision, 5*(11), 983–1003, http://journalofvision.org/5/11/5/, doi:10.1167/5.11.5. [PubMed] [Article]

Sankeralli, M. J., & Mullen, K. T. (2001). Bipolar or rectified chromatic detection mechanisms? *Visual Neuroscience, 18,* 127–135. [PubMed]

Sasaki, Y., & Watanabe, T. (2004). The primary visual cortex fills in color. *Proceedings of the National Academy of Sciences of the United States of America, 101,* 18251–18256. [PubMed] [Article]

Schiller, P. H. (1992). The ON and OFF channels of the visual system. *Trends in Neurosciences, 15,* 86–92. [PubMed]

Shapley, R., & Reid, R. C. (1985). Contrast and assimilation in the perception of brightness. *Proceedings of the National Academy of Sciences United States of America, 82,* 5983–5986. [PubMed] [Article]

Spehar, B., & Zaidi, Q. (1997). New configurational effects on perceived contrast and brightness: Second-order White's effects. *Perception, 26,* 409–417. [PubMed]

Sterne, J. A., & Davey Smith, G. (2001). Sifting the evidence—what's wrong with significance tests? *British Medical Journal, 322,* 226–231. [PubMed] [Article]

Vladusich, T., Lucassen, M. P., & Cornelissen, F. W. (2006). Do cortical neurons process luminance or contrast to encode surface properties? *Journal of Neurophysiology, 95,* 2638–2649. [PubMed]

White, M. (1979). A new effect of pattern on perceived lightness. *Perception, 8,* 413–416. [PubMed]

Whittle, P. (1994). Contrast brightness and ordinary seeing. In A. Gilchrist (Ed.), *Lightness, brightness, and transparency*. Hillsdale, NJ: Lawrence Erlbaum Associates.

Zaidi, Q., Yoshimi, B., Flanigan, N., & Canova, A. (1992). Lateral interactions within color mechanisms in simultaneous induced contrast. *Vision Research, 32,* 1695–1707. [PubMed]

Zhou, H., Friedman, H. S., & von der Heydt, R. (2000). Coding of border ownership in monkey visual cortex. *The Journal of Neuroscience, 20,* 6594–6611. [PubMed] [Article]